



**UNIVERSIDAD
DE GRANADA**

**Past, present and future of the research performed
by the Atmospheric Physics Group of the
University of Granada**

Juan Luis Guerrero-Rascado

Department of Applied Physics, University of Granada, 18071, Granada, Spain

Andalusian Institute for Earth System Research (IISTA-CEAMA), University of Granada,
Autonomous Government of Andalusia. 18006, Granada, Spain



UNIVERSIDAD
DE GRANADA



Universidade de São Paulo (Brasil)

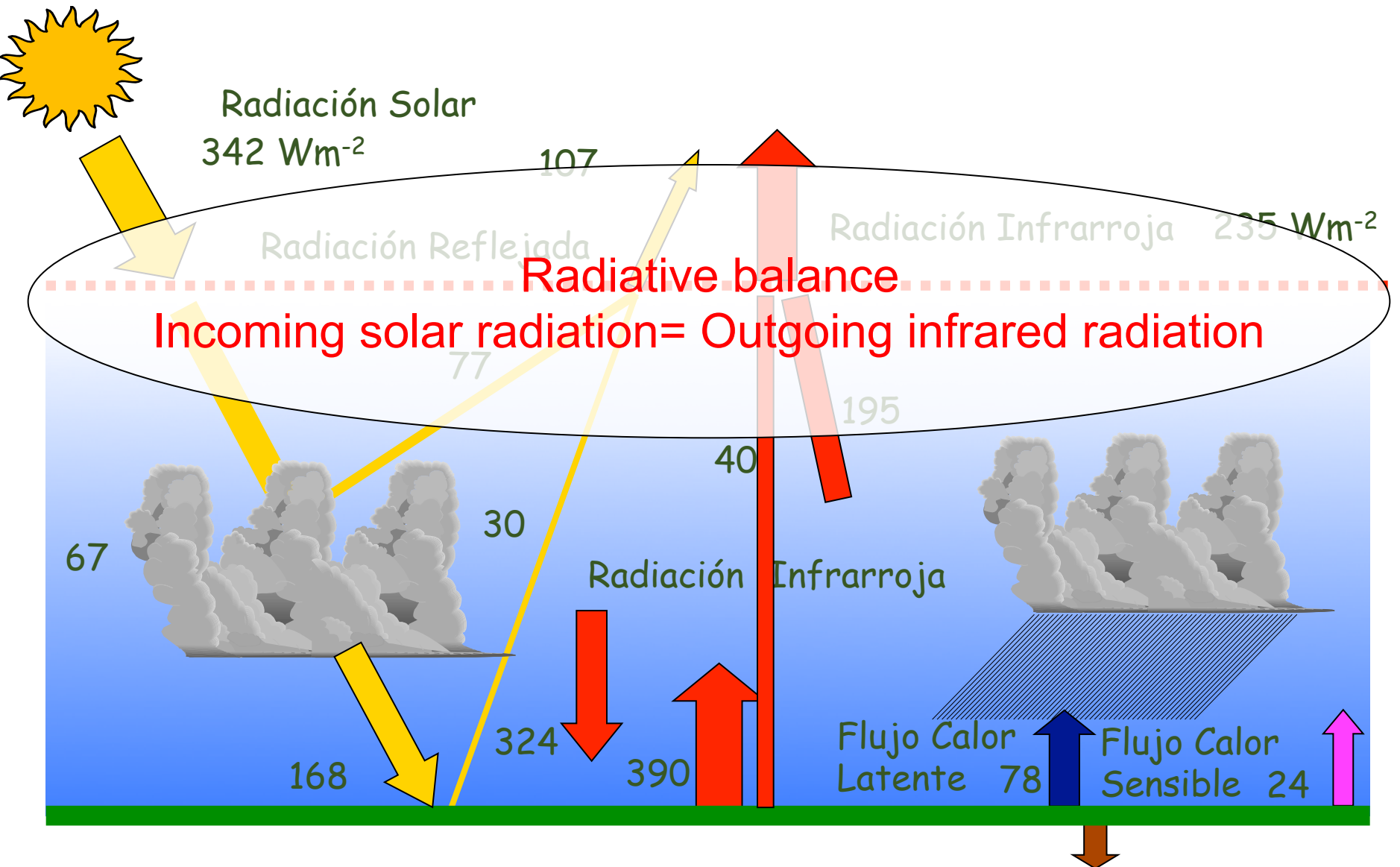
17/08/2018

Global Warming



A Planet Afflicted by a High Fever?

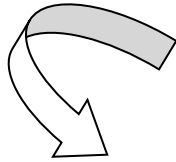
Earth System Energy Balance



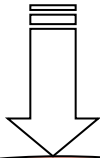
CLIMATE CHANGE

CLIMATE FORCING

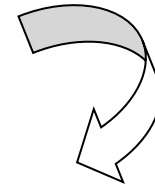
Change in the energy balance of the Earth system



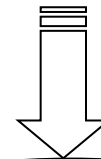
Positive Forcing



Earth surface and lower atmosphere HEATING



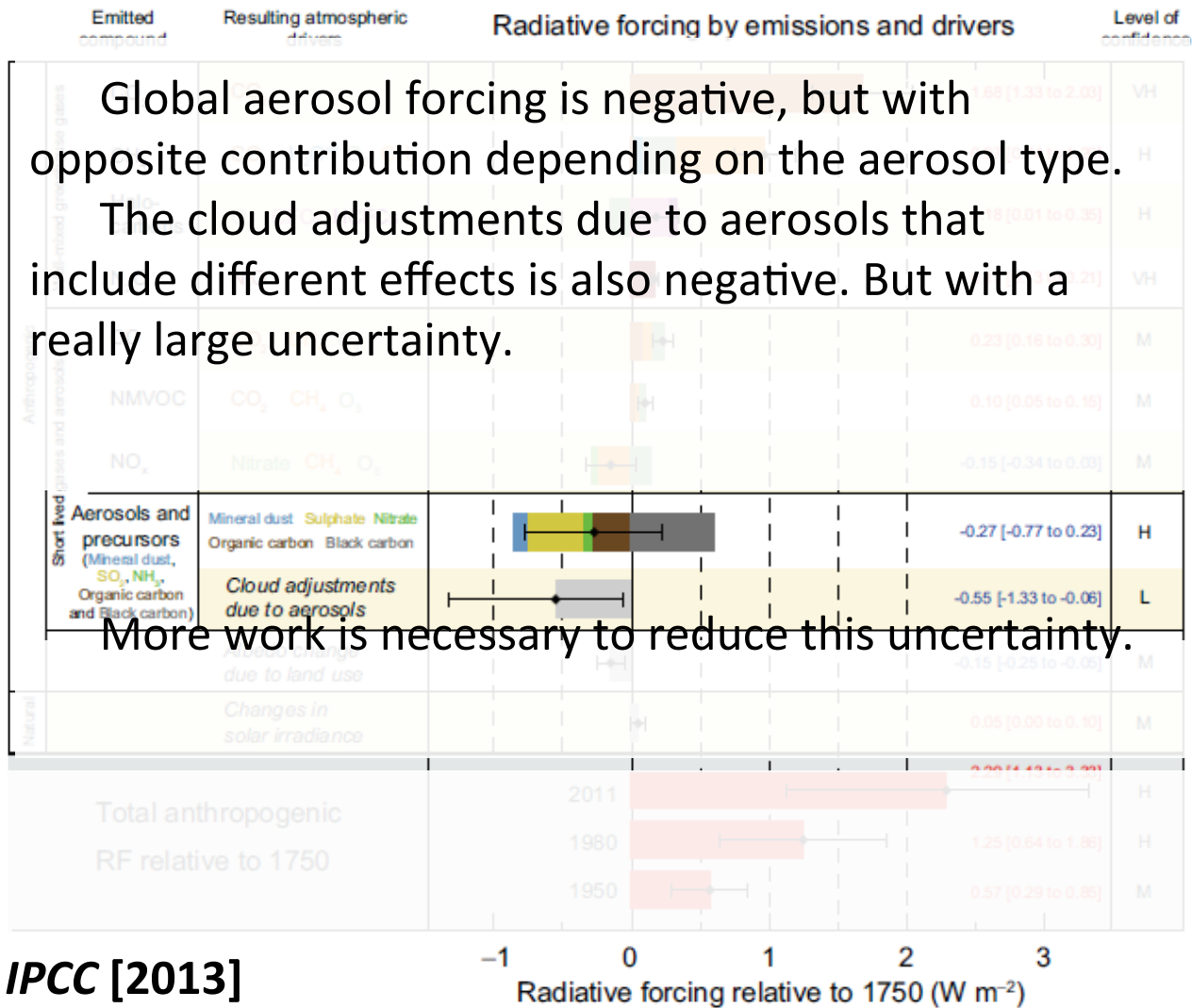
Negative Forcing



Earth surface and lower atmosphere COOLING



Atmospheric Aerosol and Climate



ATMOSPHERIC PHYSICS GROUP (UGR)

Aerosols, clouds and atmospheric radiation

Aerosols

In situ:

APS

MAAP

Nephelometer

Ultrafine Particle Monitor

PM10 & PM1 samplers

Dustrak

Hirst sampler

Remote sensing:

Sun-photometer

Star-photometer

Multiwav. Raman lidar

Scanning lidar

Clouds

All-sky imager

Scanning lidar

Sun-photometers

Ceilometer

Cloud radar

Radiation

Multi-Filter

Rotating

Shadowband

Radiometer

Bentham

Meteo.

Variables

Meteo. Sensors

Microwave radiometer

Radiosoundings

Doppler lidar

Monitoring of greenhouse gas exchanges between terrestrial ecosystems and the atmosphere

Climate variability and Climate Change

CO₂ and H₂O fluxes towers including:

Anemometers, hygrometers, open-path infrared gas analyser , etc

Climate variability and Climate Change

Team:

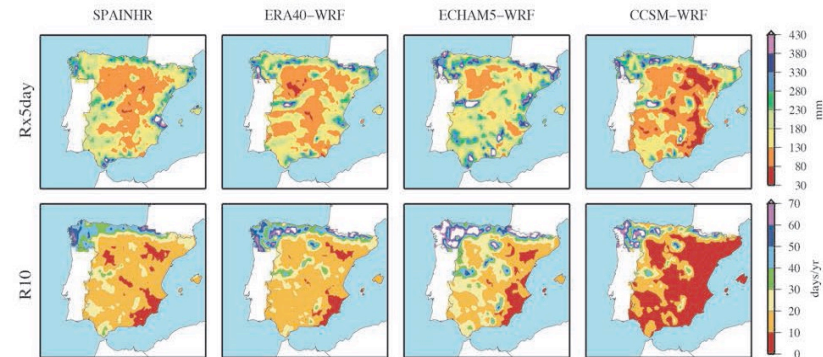
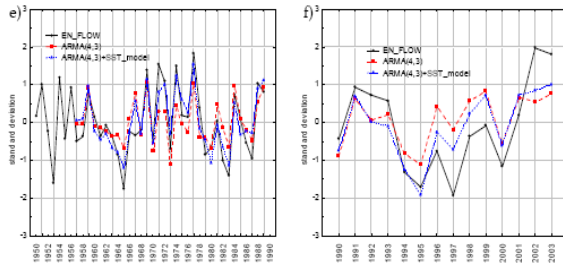
Prof. Yolanda Castro Díez
Prof. María Jesús Esteban Parra
Prof. Sonia Raquel Gámiz Fortis
Some PhD. students

What do we do?

- ❑ Causal mechanisms and sources of climate predictability in Europe (Iberian Peninsula) and Colombia
- ❑ Obtaining regional climate change projections in the Iberian Peninsula and Colombia

Specifically:

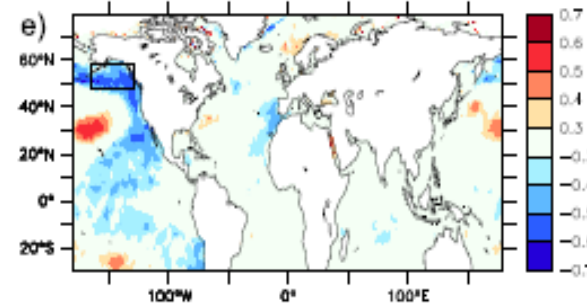
- ❑ Impacts of climate variability on the flow of rivers



- ❑ Evaluation and validation of the results of the GCMs in observational periods to determine the level of reproducibility of the current and past climatic conditions in the I.P. and Colombia.

- ❑ Statistical and dynamic downscaling (using the WRF model) of precipitation, temperature and river flow in I.P. and Colombia.

May EN_FLOW – previous spring SST



Monitoring of greenhouse gas exchanges between terrestrial ecosystems and the atmosphere

Team:

Prof. Andrew Kowalski

Prof. /researcher Penelope Serrano-Ortiz

Postdoc Enrique Pérez Sánchez-Cañete

Some PhD. students

What do we do?

Measurement of CO₂ flows and water vapor in shrubs

Abiotic flows in arid areas (ventilation processes)

Soil respiration

CO₂ exchanges in olive grove

Exchange of CH₄, CO₂ and H₂O in peatlands

Cooperation with international networks



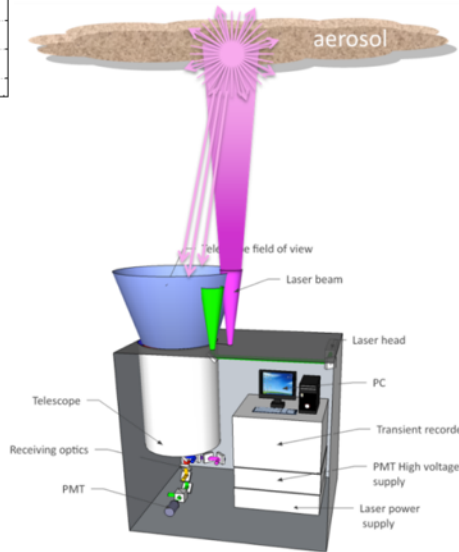
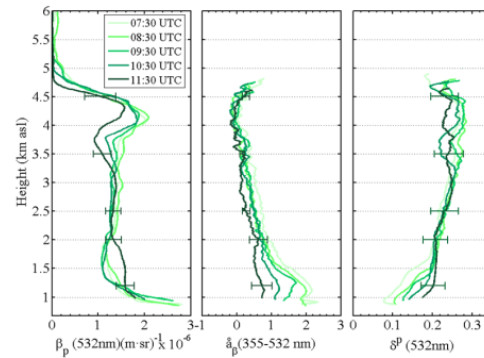
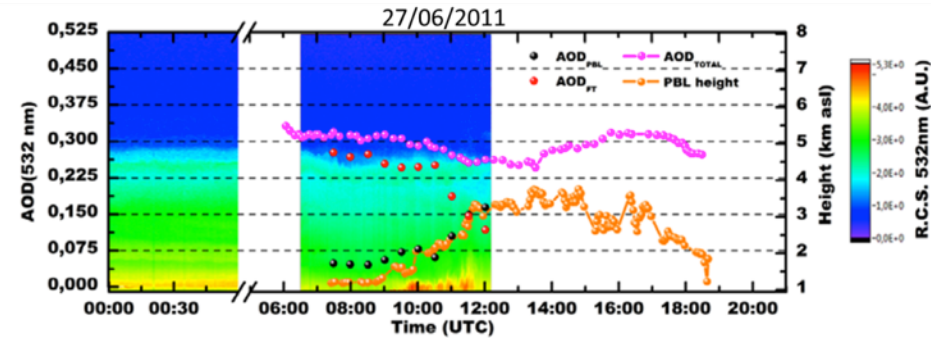
Aerosols, clouds and atmospheric radiation

Team:

Prof. Lucas Alados Arboledas
 Prof. Francisco José Olmo Reyes
 Prof. Inmaculada Foyo Moreno
 Prof. Paloma Cariñanos González
 Prof. / researcher Juan Luis Guerrero Rascado
 Researcher Hassan Lyamani
 Postdoc Alberto Cazorla Cabrera
 Postdoc Gloria Titos Vela
 Postdoc Juan Antonio Bravo Aranda
 Some PhD. Students

What do we do?

- ❑ Measurement of aerosol optical and microphysical properties
- ❑ Active and passive remote sensing of aerosols and clouds
- ❑ Coordinated observations in international networks
- ❑ Validation programs of observing satellites
- ❑ Air quality studies
- ❑ Aerosol-cloud interactions



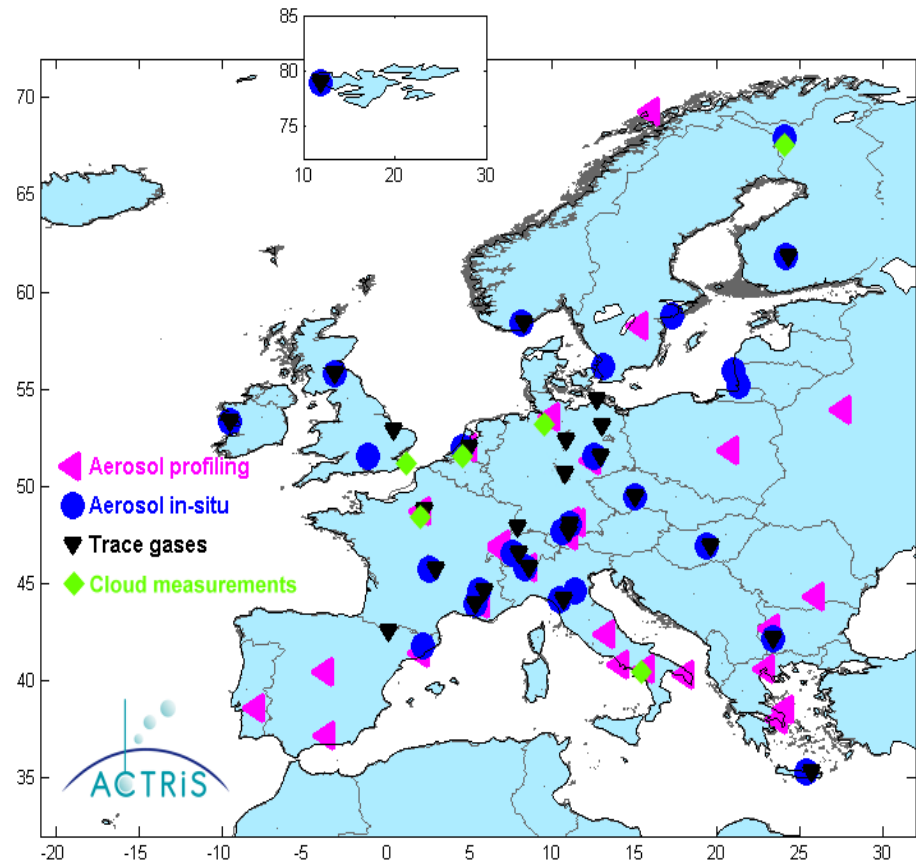
A new generation of research: ACTRIS

ACTRIS (Aerosols, Clouds, and Trace gases Research InfraStructure Network) is the integration of European ground-based stations equipped with advanced atmospheric probing instrumentation for:

- aerosols
- clouds
- short-lived gas-phase species

Building of new knowledge as well as policy issues on climate change, air quality, and long range transport of pollutants

ACTRIS is building the next generation of the ground-based component of the EU observing system by integrating three existing research infrastructures EUSAAR, EARLINET, CLOUDNET, and a new trace gas network component into a single coordinated framework.



<http://www.actris.net>

The ACTRIS objectives:

Activities distributed in Work Packages: WP1 to WP22

WP n°	WP Title	WP Leader	
WP 1	NA1: ACTRIS Management and coordination	CNR	Gelsomina Pappalardo
WP 2	NA2: Remote sensing of vertical aerosol distribution	UPC	Adolfo Comeron
WP 3	NA3: In-situ chemical, physical and optical properties of aerosols	IFT	Alfred Wiedensohler
WP 4	NA4: Trace gases networking: Volatile organic carbon and nitrogen oxides	EMPA	Stefan Reimann

...

.....

.....

....

WP 20	JRA1: Lidar and sunphotometer – Improved instruments, integrated observation strategies and algorithms for the retrieval of advanced aerosol microphysical products	IFT	Ulla Wandinger
WP 21	JRA2: Comprehensive gas phase and aerosol chemistry	PSI	Urs Baltensperger
WP 22	JRA3: A framework for cloud-aerosol interaction studies	TUD	Herman Russchenberg

One past project ...

Project: 3D Atmospheric aerosol regional monitoring by combination of multiwavelength lidar and ceilometer-radiometer network (TRIAEROMONITOR)

The GENERAL OBJECTIVE of this project will be the advancement in the 3D regional monitoring of atmospheric aerosol. In this way, and using some available instruments, regionally distributed, we propose the development of network for 3D characterization of atmospheric aerosol by combination of a core station including a high performance lidar and distributed stations equipped with sun and sky radiometers and ceilometers.

SPECIFIC OBJECTIVES:

1. Improvement in aerosol characterization by means of passive and active remote sensing.
2. Implementation of analysis procedures for deriving aerosol optical profiles from ceilometers.
3. Development of network for 3D characterization of atmospheric aerosol by combination of high performance lidar, sun and sky radiometers and ceilometers.
4. 3D regional characterization of the atmospheric aerosol during medium-long range transport.

Cazorla, A., et al.: Near-real-time processing of a ceilometer network assisted with sun-photometer data: monitoring a dust outbreak over the Iberian Peninsula, *Atmos. Chem. Phys.*, 17, 11861-11876, <https://doi.org/10.5194/acp-17-11861-2017>, 2017

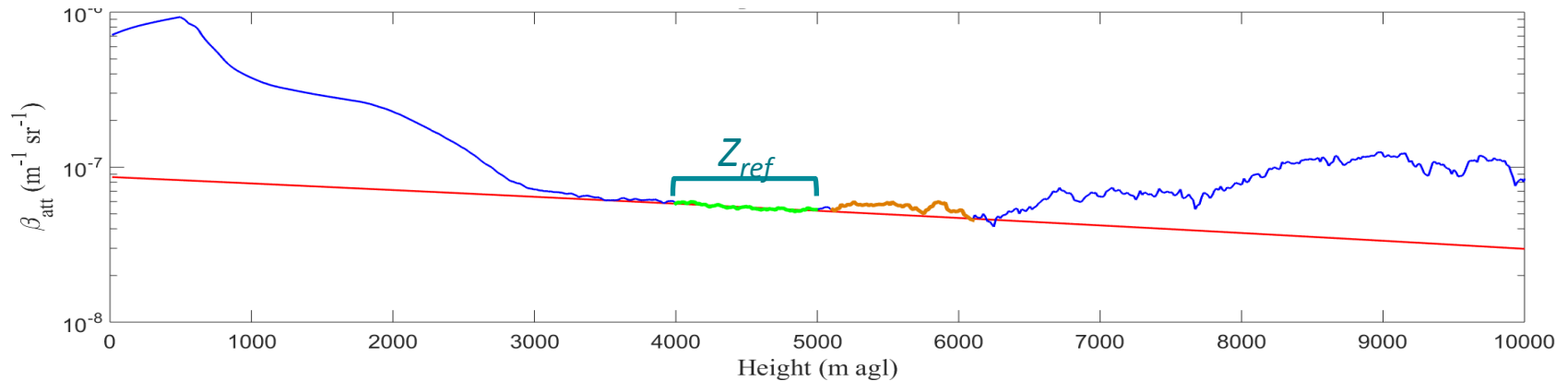
Introduction

- The interest on vertical resolved aerosol characterization with ceilometers has increased in the last few years with the development of more sensitive ceilometers.
- **Pros:**
 - Automatic and much simpler operation compared to lidars
 - Lower cost
 - Possibilities for better spatial and temporal resolution
- **Cons:**
 - Reduced signal to noise ratio (difficult to extract optical aerosol properties)
- A distributed network of ceilometer has been set up
 - Using common calibration and data analysis procedures
 - The inversions obtained with ceilometer are compared with independent lidar inversion with a multiwavelength Raman Lidar (Granada station)
 - A strong dust event on February 20-24 2016 was visible in all stations and it has been used for testing.
 - Data from the station in Granada has been used for model evaluation

Ceilometers: calibration process

$$P(z) = C_L \cdot \frac{O(z)}{z^2} \beta(z) \cdot T^2(z) \quad \text{RCS}(z) = P(z) \cdot z^2 \quad \beta_{\text{att}}(z) = \beta(z) \cdot T^2(z)$$

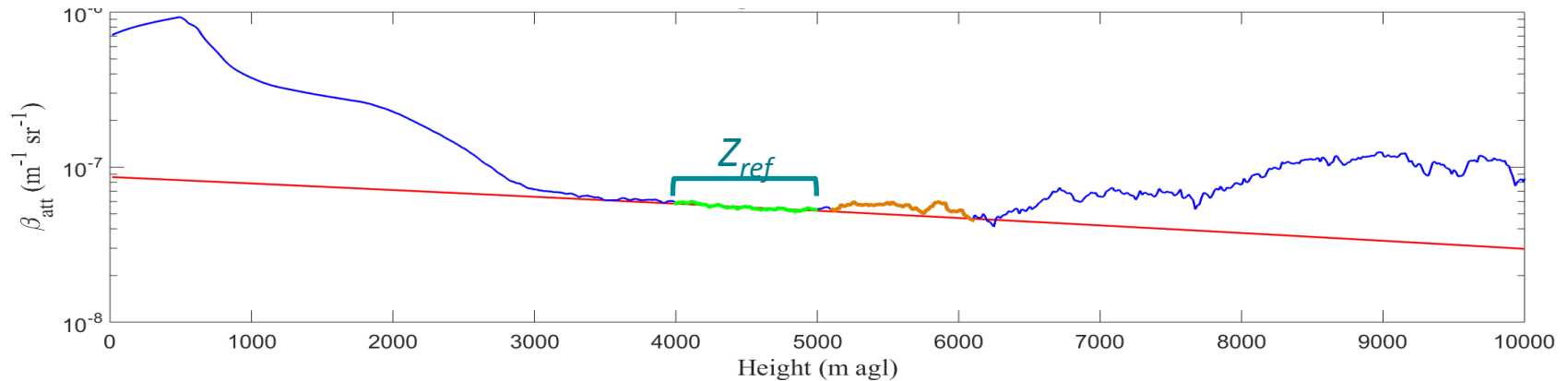
measurement goal



1. Temporal averaging of the profiles is performed (hourly averages are used for the calibration). The first 300m of the profile are assigned to the value at 300m to avoid large overlap correction
2. For each profile a set of potential z_{ref} is obtained by comparing the profiles of the RCS and β_m , which is obtained from a standard atmosphere profile scaled to ground temperature and pressure. The slopes are calculated over a 990m window. All regions with slope differences below 1% are selected.

Ceilometers: calibration process

$$P(z) = C_L \cdot \frac{O(z)}{z^2} \beta(z) \cdot T^2(z) \quad \text{measurement} \quad \text{RCS}(z) = P(z) \cdot z^2 \quad \beta_{\text{att}}(z) = \beta(z) \cdot T^2(z) \quad \text{goal}$$



3. For each z_{ref} and L_r from 20 to 80 sr, K-F inversion is applied and the resulting profile for the β_p is integrated and multiplied by the L_r and compared to the AOD. The pair z_{ref} and L_r that minimizes the difference between the integral of the α_p profile with the AOD is selected.

4. Finally, C_L is calculated (if the minimum difference calculated in step 3 is <10 %)

$$C_L(z_{\text{ref}}) = \frac{\text{RCS}(z_{\text{ref}})}{\beta_m(z_{\text{ref}}) \cdot T_m^2(z_{\text{ref}}) \cdot T_p^2(z_{\text{ref}})}$$

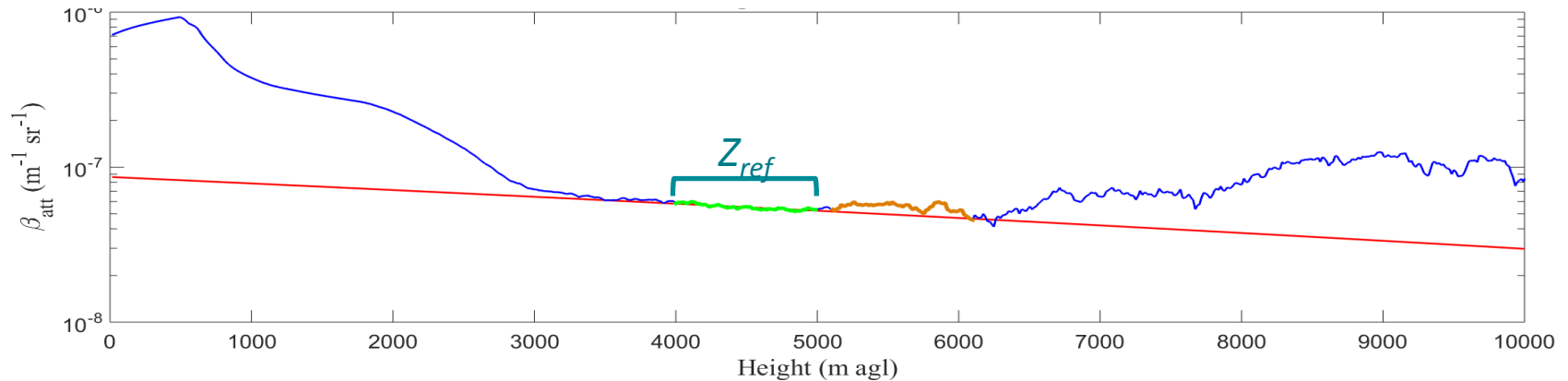
$$\text{RCS}(z) = P(z) \cdot z^2$$

$$T_p^2(z_{\text{ref}}) = e^{-2 \times \text{AOD}}$$

Ceilometers: calibration process

$$P(z) = C_L \cdot \frac{O(z)}{z^2} \beta(z) \cdot T^2(z) \quad \text{RCS}(z) = P(z) \cdot z^2 \quad \beta_{\text{att}}(z) = \beta(z) \cdot T^2(z)$$

measurement goal



So, now we can obtain CALIBRATED attenuated backscatter coefficients:

$$\beta_{\text{att}}(z) = \frac{\text{RCS}(z)}{C_L(z_{\text{ref}})}$$

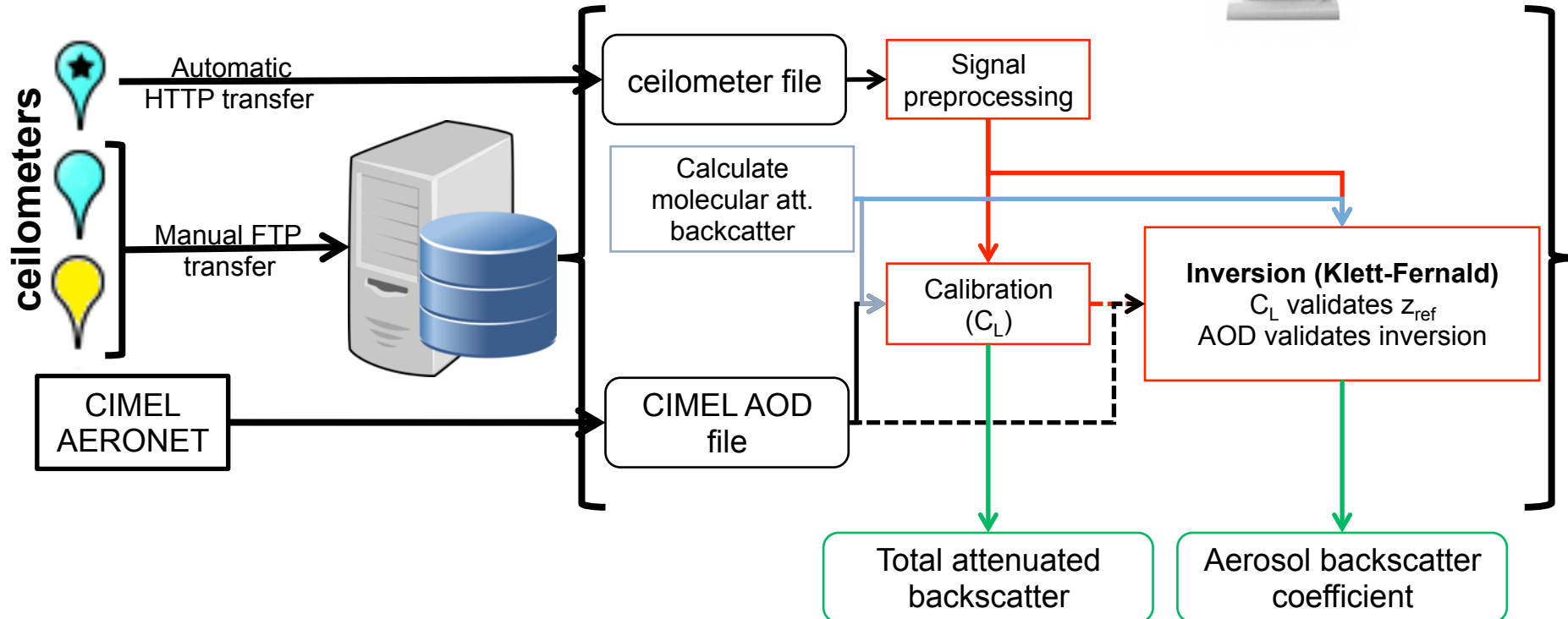
Iberian Ceilometer Network (ICENET)



Iberian Ceilometer Network (ICENET)

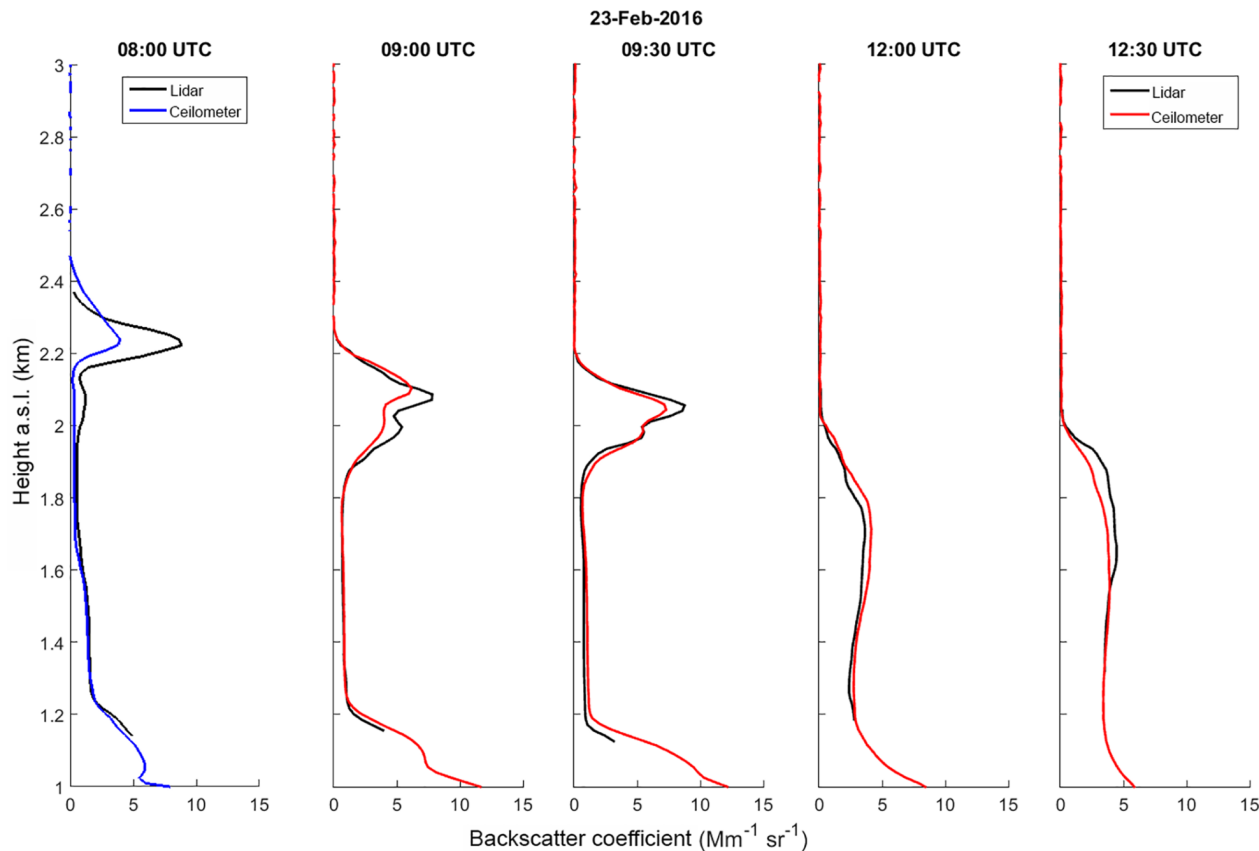
Lufft CHM 15k Nimbus

- ❑ Nd:YAG 1064nm.
- ❑ Energy/pulse: $8 \mu J$.
- ❑ Frequency of pulses: 6,5 kHz.
- ❑ Overlap > 80 % at 480 m.
- ❑ Provides overlap and background corrected backscattered signal



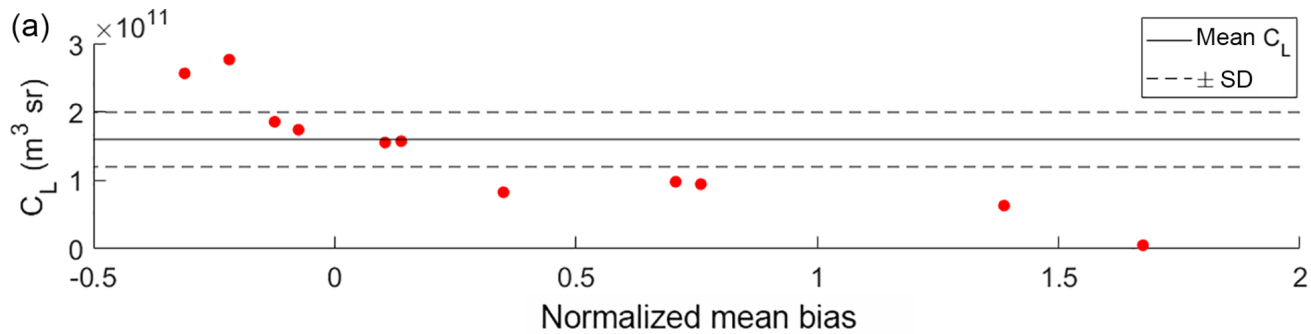
Ceilometer – Lidar comparison

- ❑ 30-min lidar elastic inversions are used to validate the ceilometer inversions
- ❑ Raman lidar LR331D400 «MULHACEN» (Raymetrics Ltd.): 1064, 607, 532 | |, 532s[⊥], 408, 387 & 355 nm
- ❑ Elastic inversion using Klett-Fernald method at 1064 nm are used, with fixed lidar ratio (50 sr)
- ❑ Coherence checked against Klett-Fernald and Raman methods at 355 and 532 nm

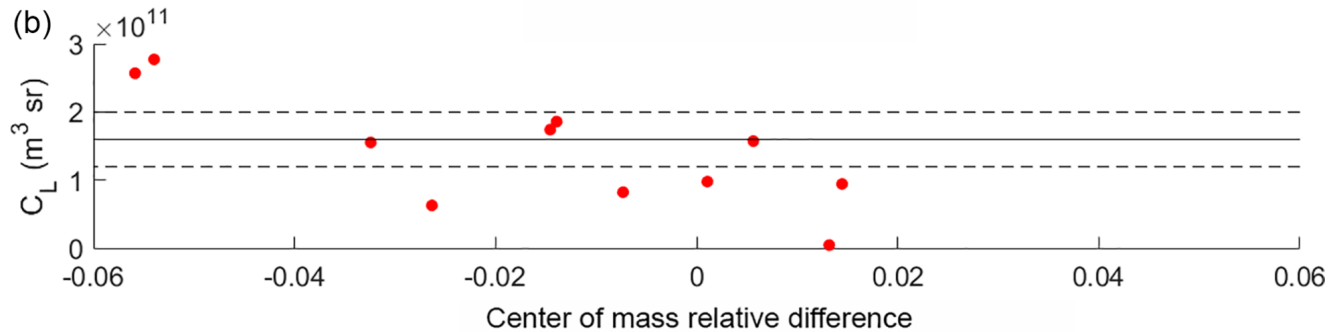


Lidar and ceilometer particle backscatter profiles for five cases on 23 February 2016. The first case (marked in blue) is a rejected ceilometer profile and the other four cases (marked in red) are cases with a ceilometer calibration factor within the 33% of the median CL

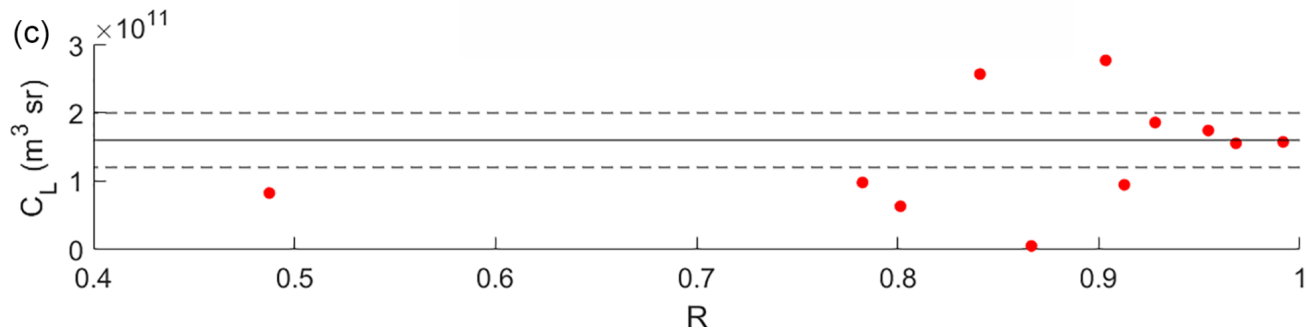
Ceilometer – Lidar comparison



$$\text{NMB} = \frac{\bar{\beta}_{\text{ceil}} - \bar{\beta}_{\text{lidar}}}{\bar{\beta}_{\text{lidar}}}$$

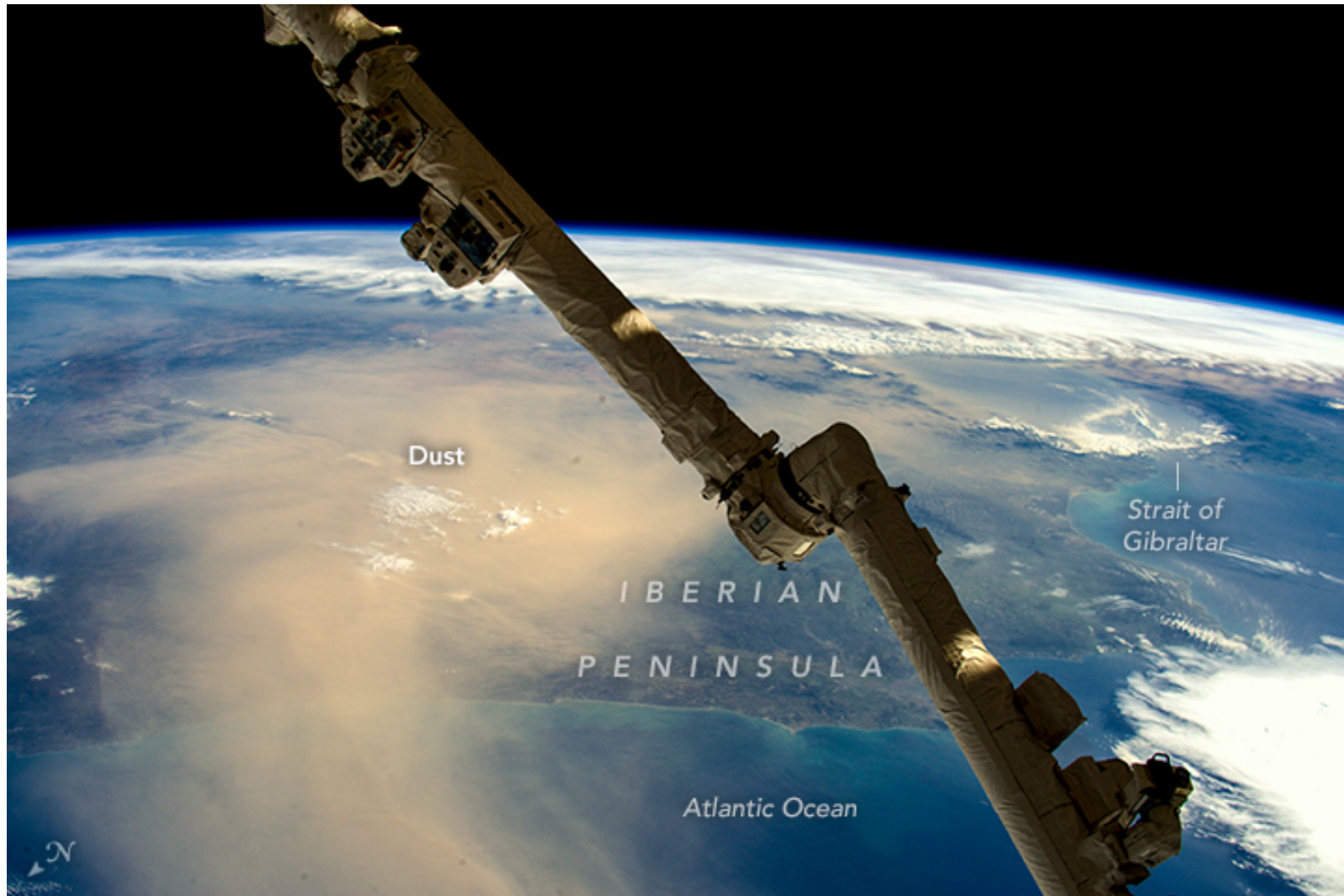


$$C_{\text{mass}} = \frac{\int_{z_{\text{min}}}^{z_{\text{max}}} z \cdot \beta(z) dz}{\int_{z_{\text{min}}}^{z_{\text{max}}} \beta(z) dz}$$



Ceilometer calibration factor (C_L) vs. normalized mean bias (NMB) (a), relative difference in center of mass (b) and coefficient of correlation (R) (c). The solid horizontal line indicates the mean C_L for the dust event period and dashed lines indicate the 33% around this mean value.

The dust event



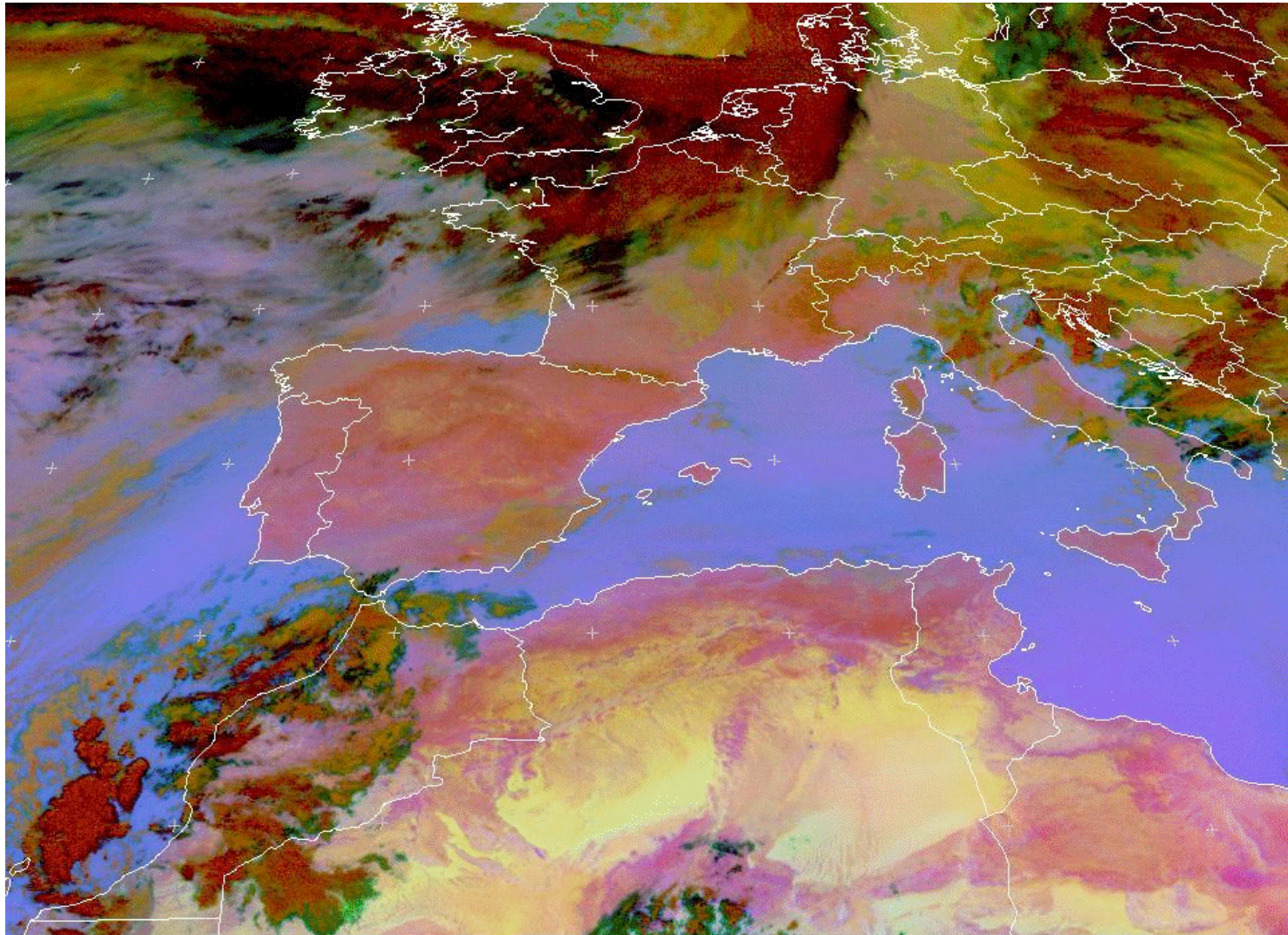
Tim Peake, International Space Station (February 21)

The dust event



MODIS Aqua (February 21, 14 UTC)

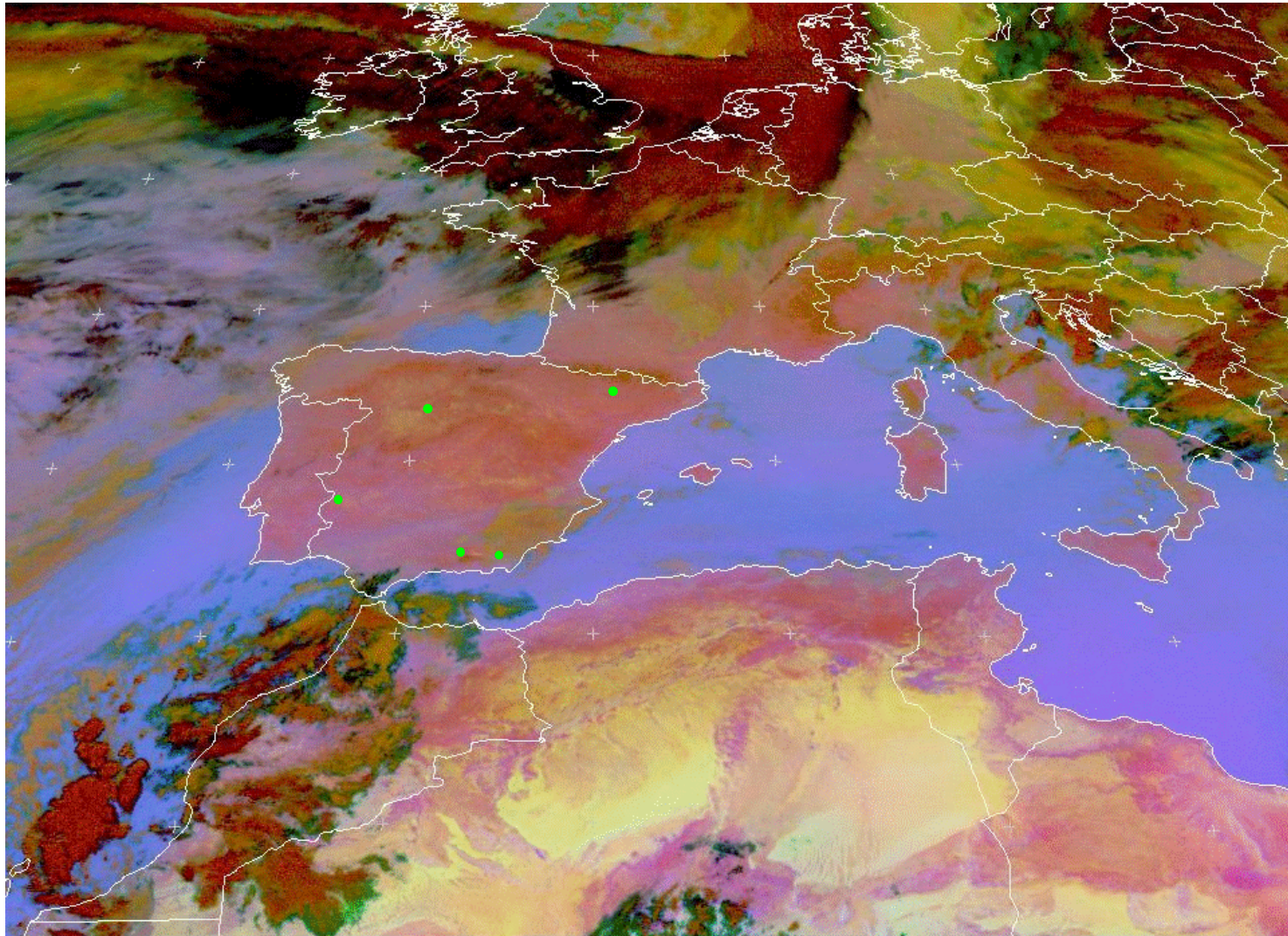
The dust event



Met10 RGB-Dust 2016-Febr-20 00 UTC

 EUMETSAT

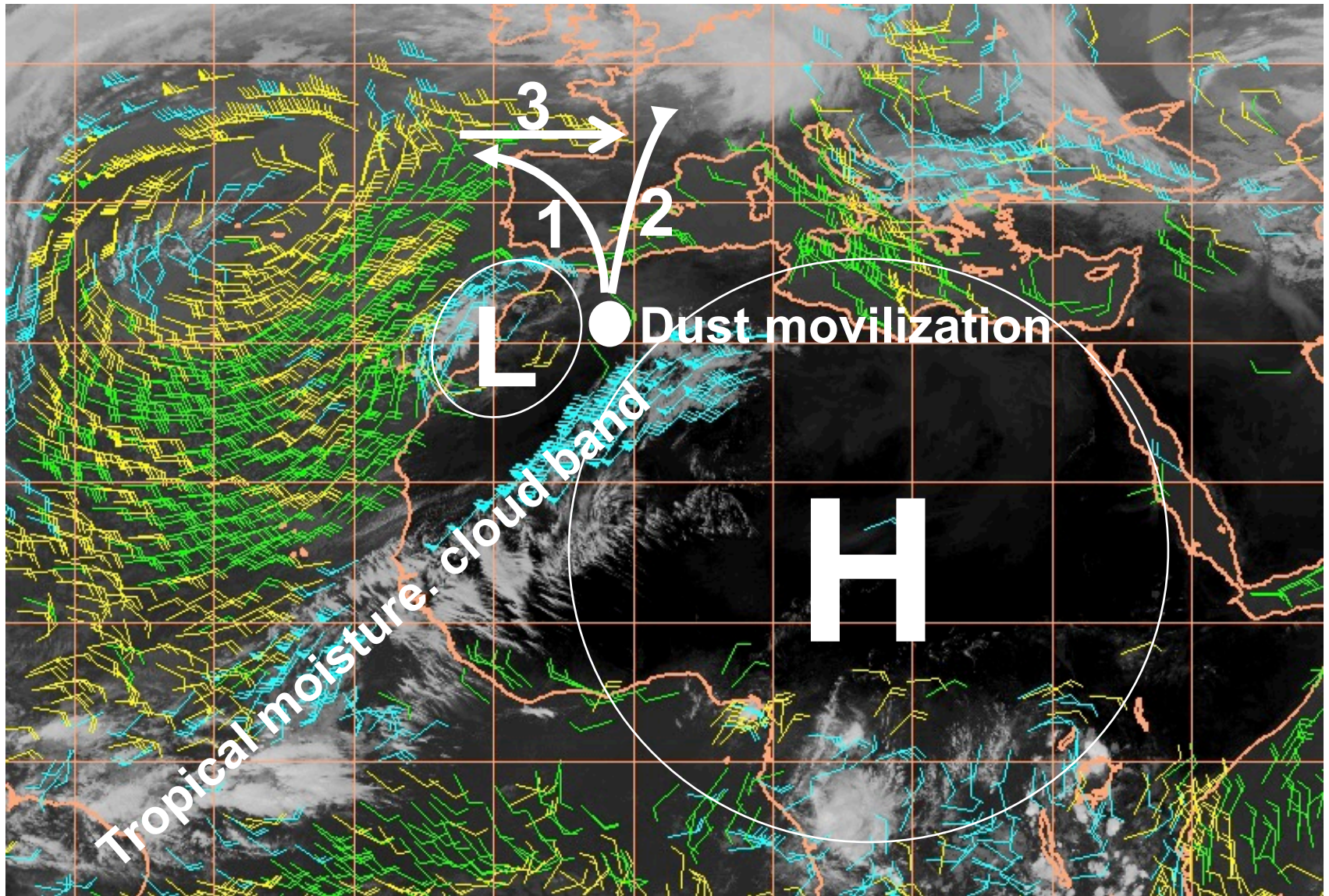
The dust event

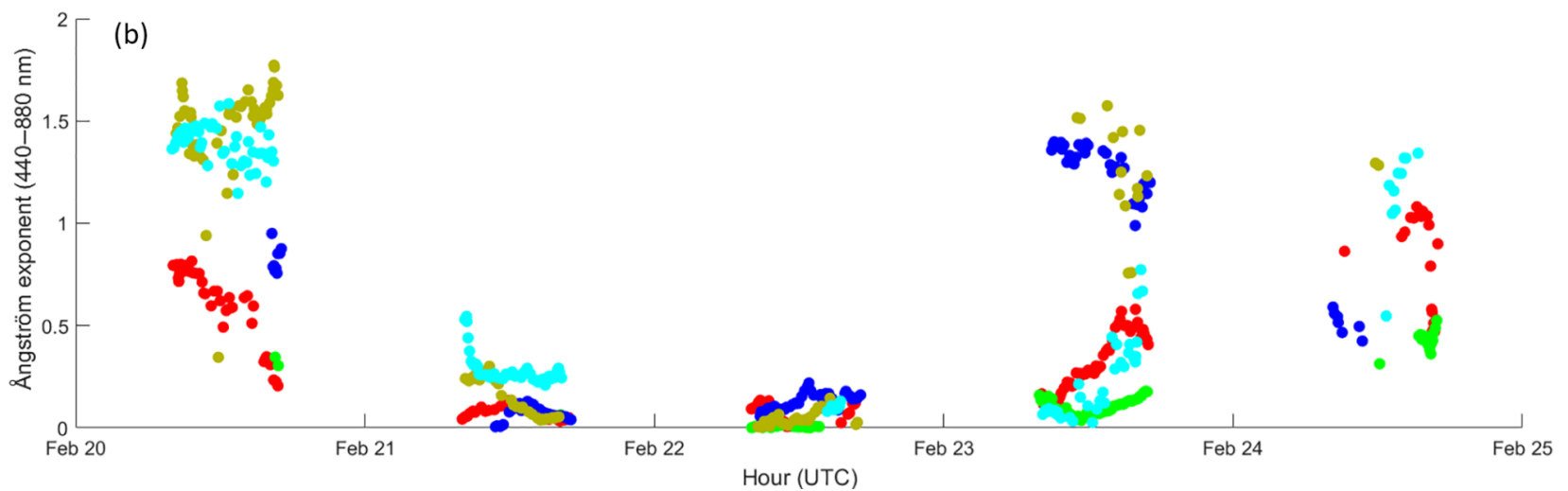
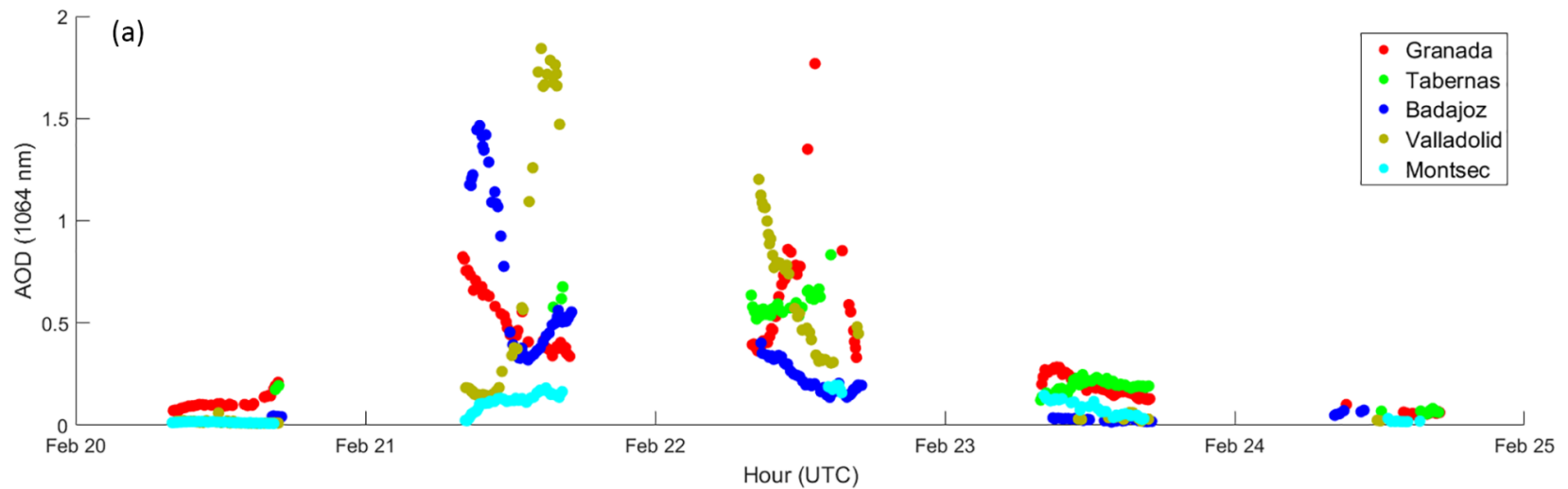


Met10 RGB-Dust 2016-Febr-20 00 UTC

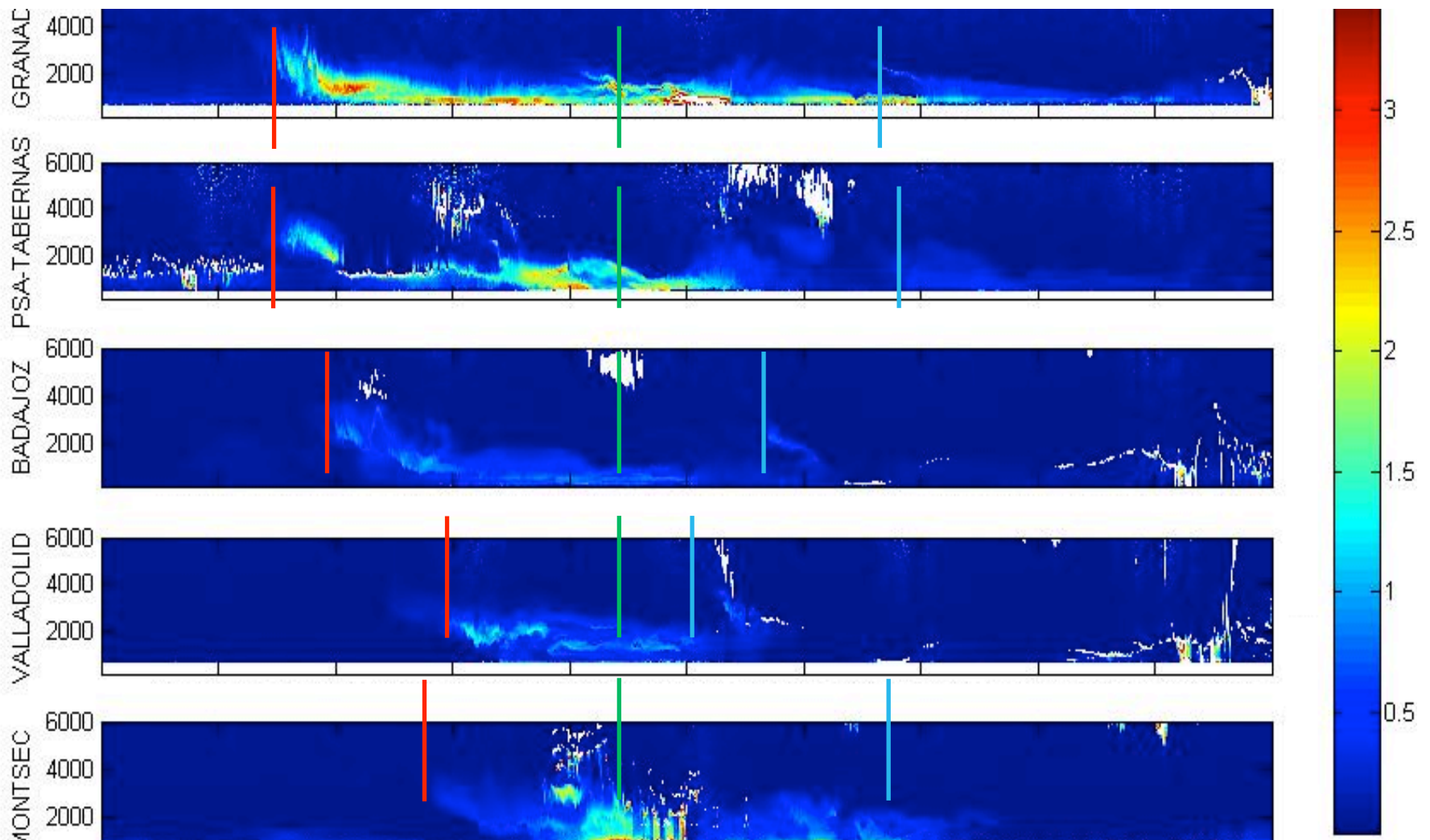
 EUMETSAT

The dust event

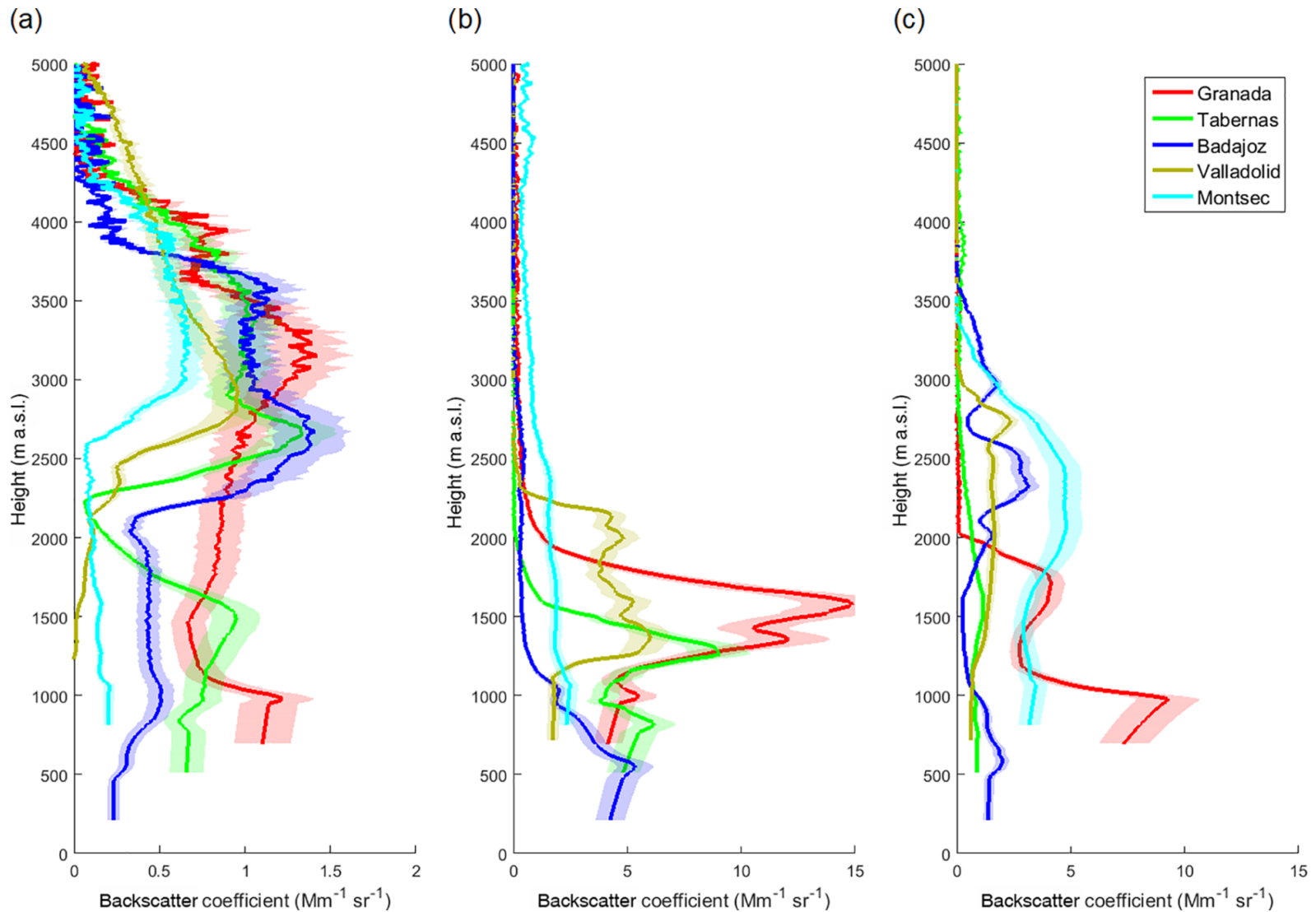




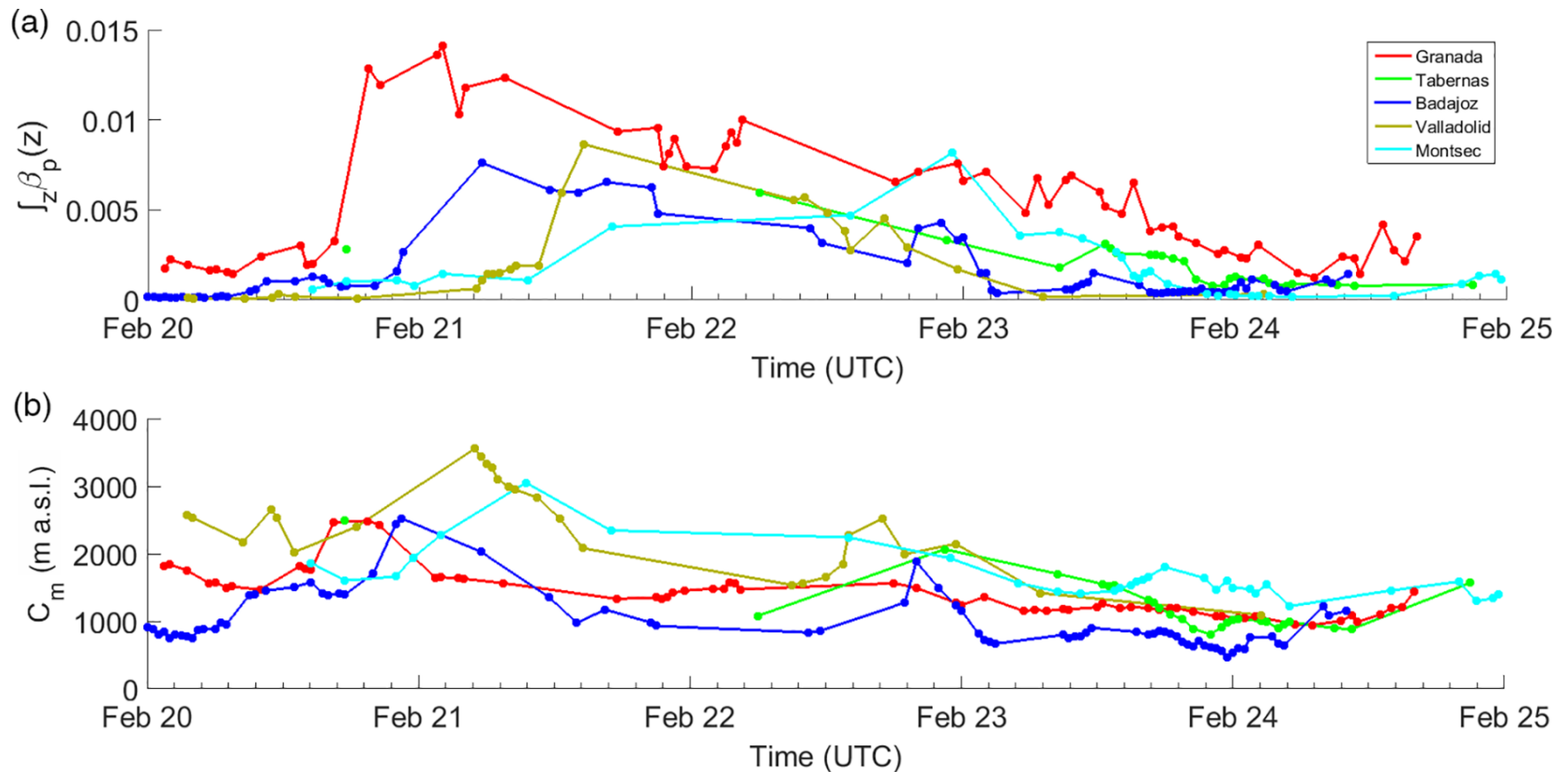
Sun-photometer time series representing the AOD at 1064 nm (a) and Ångström exponent between 440 and 800 nm (b) for all sites in ICENET during the dust event.



Ceilometer time series of total attenuated backscatter representing the evolution of the dust outbreak between 20 and 24 February 2016 (the color scale is logarithmic)



Particle backscatter coefficient profiles for all stations at the beginning (a), middle (b) and final stage (c) of the outbreak (note that the x axis has a different scale and the profiles start at ground level). The shaded areas represent the 15% uncertainty.



Time series of the integral of the particle backscatter coefficient for all stations (a) and time series of the center of mass of the backscatter profiles for all stations (b).

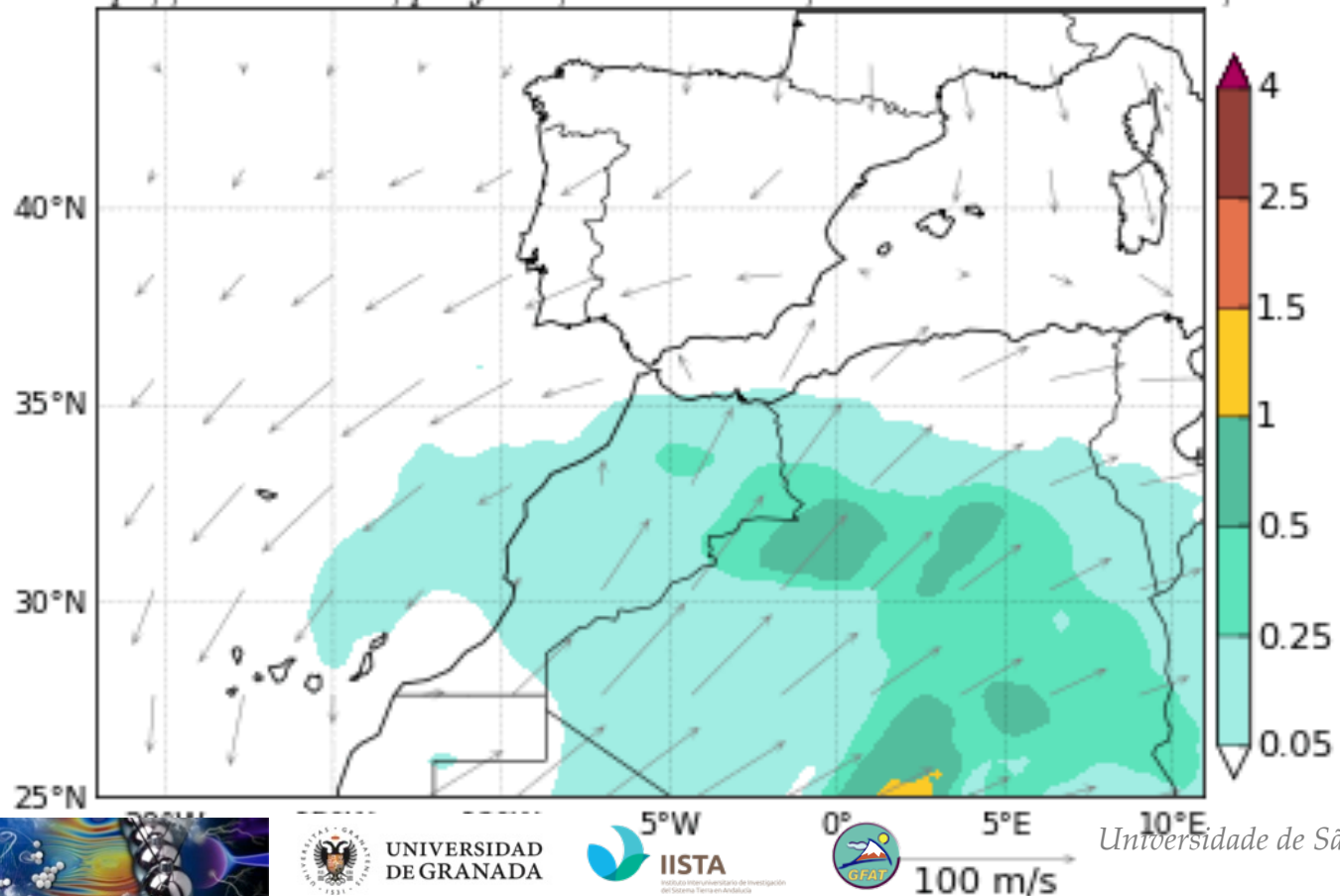
Model Evaluation

NMMB-BSC Dust Forecast

- Prediction of the atmospheric life cycle of the eroded desert dust for a regional and global domain
- Provides dust forecast for the WMO Sand and Dust advisory and assessment system
- The model evaluation is needed in near real time

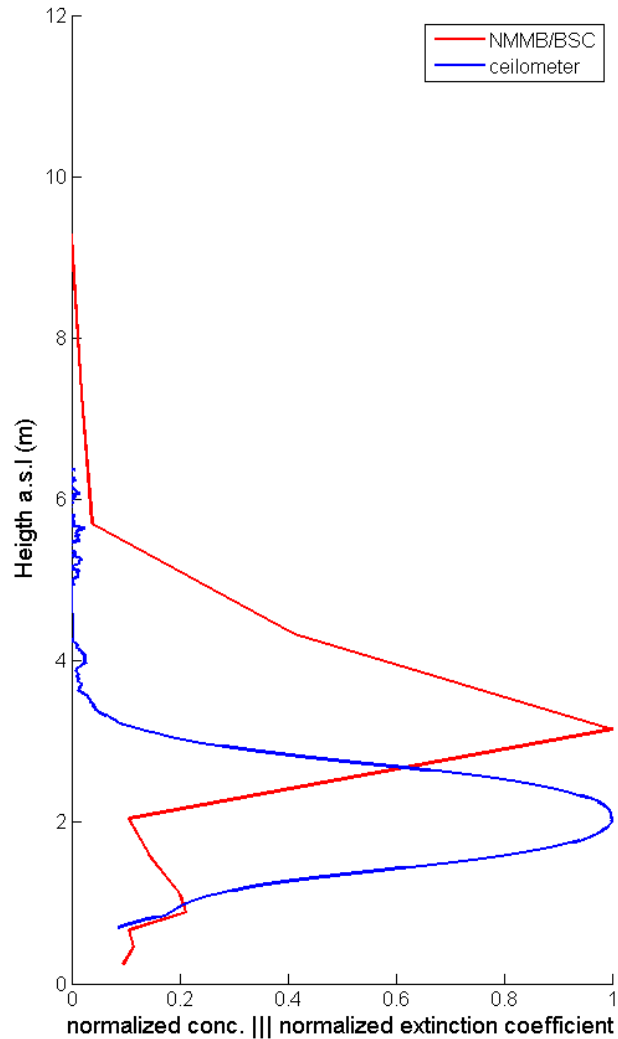
NMMB/BSC-Dust Dust Load (g/m^2) and 700 hPa Wind
00h forecast for 12UTC 20 Feb 2016

<http://www.bsc.es/projects/earthscience/NMMB-BSC-DUST/>

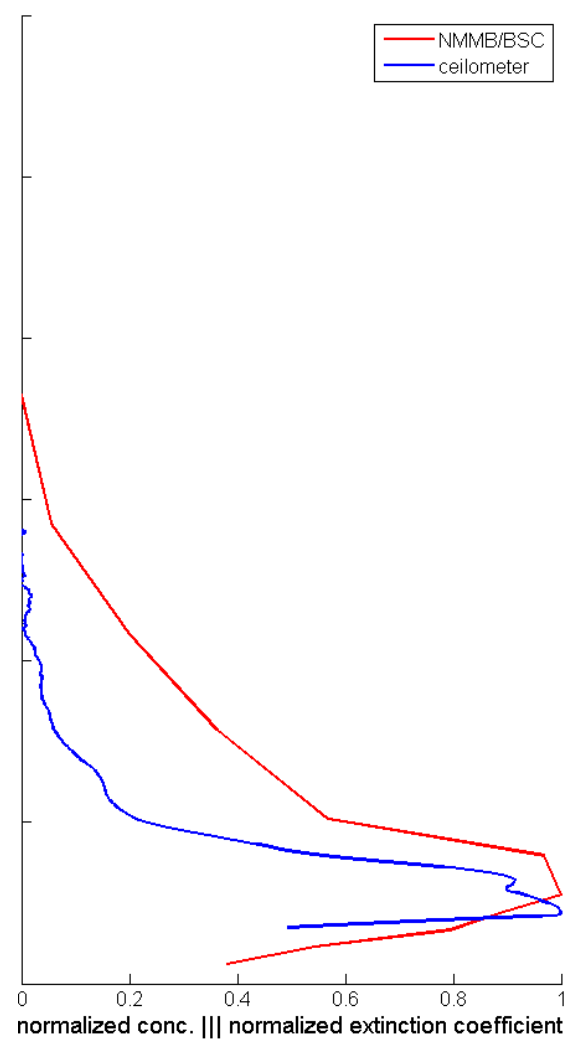


Model Evaluation

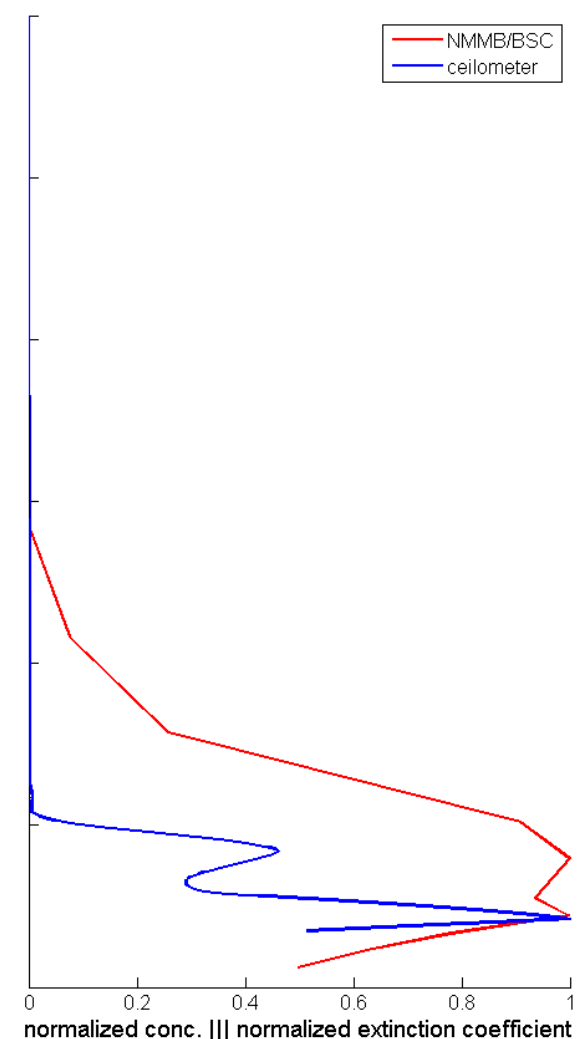
20-Feb-2016 18:00



22-Feb-2016 00:00



23-Feb-2016 12:00



Conclusions

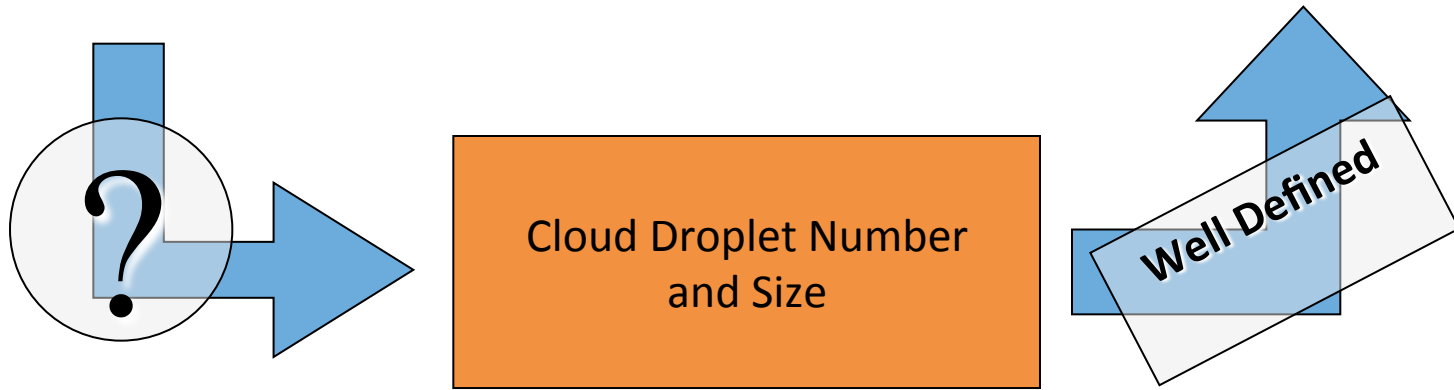
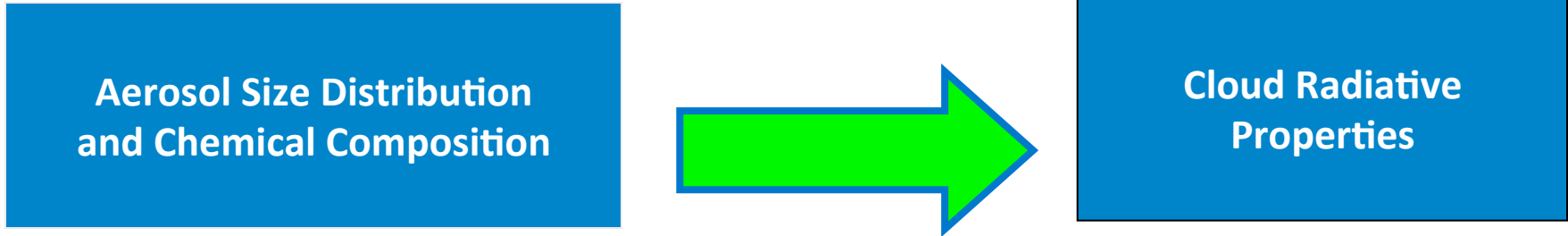
The Iberian ceilometer network provides automated total attenuated backscatter profiles by routinely calibrating the signal and performs inversion of backscattered profiles in order to obtain particle backscatter coefficient profiles with the aid of CIMEL AOD data.

- Particle backscatter coefficient profiles give a quantitative way to characterize singular events allowing multi-site monitoring of events in near real time.
- A Lidar comparison during a dust event provided an estimation of about
 - ❑ Up to 20% difference between ceilometer and lidar particle backscatter coefficient profiles
 - ❑ Less than 2% difference in the center of mass of the profile
- The ceilometer network can be used for model evaluation
 - ❑ Multiple profiles are provided by the network and distributed over a large region
 - ❑ Quality of the ceilometer profiles can be evaluated automatically in NRT
 - ❑ Model output can be directly compared to ceilometer profiles

One present project ...



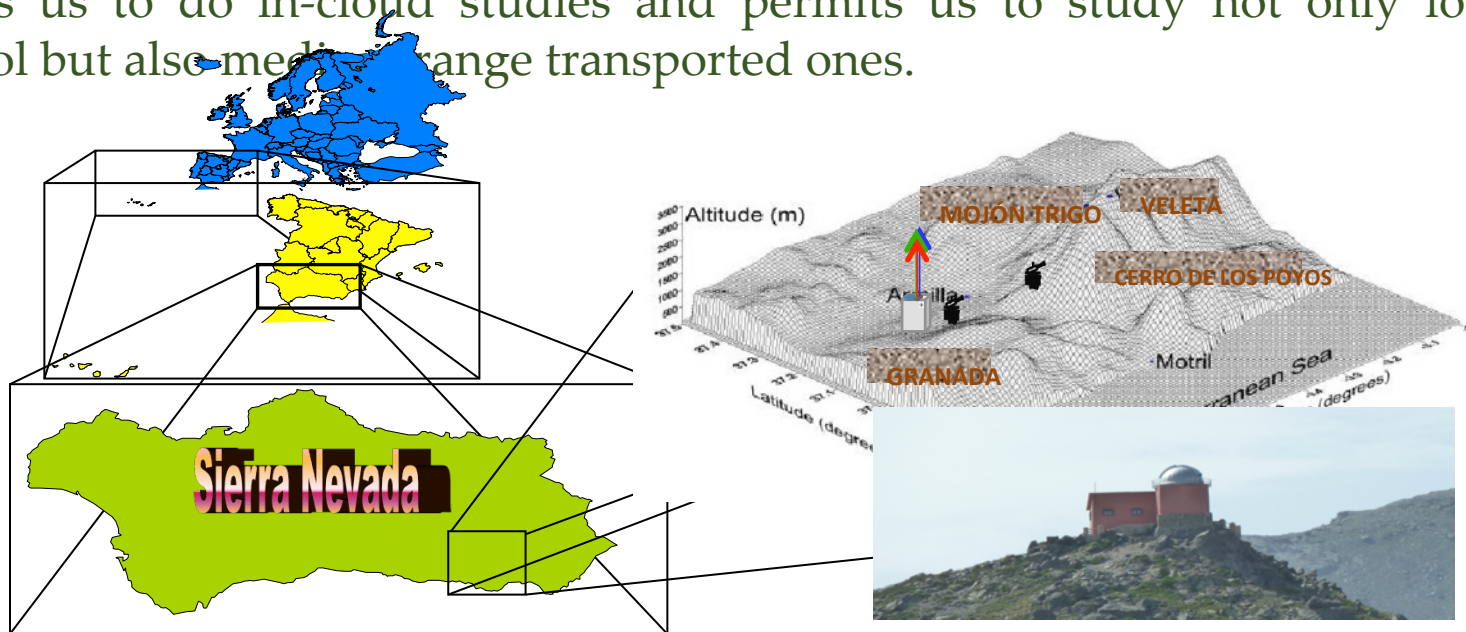
OPEN ISSUE



Empirical relationships are needed!

Project: CLOUD Aerosol Radiation Interaction (CLARIN)

- CLARIN will explore direct ground based remote sensing methods to assess the Aerosol-Cloud Interaction directly, different remote sensing tools will be used in a synergetic way.
- To address the aerosol-cloud interaction processes in detail, properties such as size, composition and mixing state of the individual particles need to be known.
- In this project we will address this issue using a high mountain station that allows us to do in-cloud studies and permits us to study not only local aerosol but also medium range transported ones.



Project: CLOUD Aerosol Radiation Interaction (CLARIN)

The GENERAL OBJECTIVE of this project is contributing to increasing the knowledge of the role of the atmospheric aerosol in the Earth's climate, thus reducing the uncertainties associated to Cloud, Aerosol, Radiation Interaction. Using remote sensing atmospheric profiling and in-situ techniques, alone in a synergetic approach.

SPECIFIC OBJECTIVES:

- Optimization of the remote sensing profiling.
- Exploring different alternatives for the study of aerosol cloud interaction, ACI, using ground based remote sensing. This will include the characterization of the atmospheric aerosol and the clouds using a combination of active and passive remote sensing instruments.
- Study ACI by in-situ aerosol and cloud measurements at a high mountain observatory.
- Use the combination of different remote sensing techniques for the study of the changes in the aerosol optical properties in the so-called twilight zone, including the characterization of the columnar volume size distribution on the atmospheric aerosols in the vicinity of clouds.

Aerosol Cloud Interaction, ACI_x , where $x \in \{\tau_d, r_e, N_d\}$ can be defined by the following equalities [Feingold et al., 2001], where α is an observed proxy for aerosol amount :

$$ACI_\tau = \left. \frac{\partial \ln \tau_d}{\partial \ln \alpha} \right|_{LWP} \quad 0 < ACI_\tau < 0.33 \quad (1a)$$

$$ACI_r = - \left. \frac{\partial \ln r_e}{\partial \ln \alpha} \right|_{LWP} \quad 0 < ACI_r < 0.33 \quad (1b)$$

$$ACI_N = \frac{d \ln N_d}{d \ln \alpha} \quad 0 < ACI_N < 1.0 \quad (1c)$$

$$ACI_\tau = -ACI_r = \frac{1}{3} ACI_N \quad (1d)$$

cloud optical depth τ_d , cloud droplet effective radius r_e , and cloud droplet number concentration N_d

The aerosol and cloud properties required for quantifying ACI as in equation will be measured by a suite of instruments and are summarized in the following table:

Cloud Liquid water content	LWC (gm^{-2})	Cloud Droplet Probe CDP2
Cloud optical depth	τ_d	Multi-filter Rotating Shadowband Radiometer MFRSR Sun-photometer Lidar
Cloud droplet effective radius	R_e (μm)	Cloud Droplet Probe CDP2, Derived Derived from MFRSR, MWR Derived from Sun-photometer, MWR Derived from lidar, MWR Derived from Cloud Droplet Radar, MWR
Cloud updraft velocity	w (ms^{-1})	Sonic Anemometer Doppler lidar
Cloud droplet number concentration	N_d (cm^{-3})	Cloud Droplet Probe CDP2, MWR Derived from Cloud Droplet Radar, MWR
Aerosol extinction	σ_e (m^{-1})	Lidar
Aerosol Size distribution	N_a (cm^{-3})	SMPS

WORK PACKAGES

WP 1. Aerosol Cloud Interaction based on in-situ measurements in a high mountain station

WP 2. Aerosol Cloud Interaction, ACI, base on ground-based remote sensing

WP 3. Comparison and synergies between in-situ and ground surface remote sensing for ACI determination

WP 2. Aerosol Cloud Interaction, ACI, base on ground-based remote sensing

T.2.1 ACI by combination of MWR, MWRLIDAR, CIMEL, DOPPLER LIDAR. (T1-T4)

T.2.2. ACI from MWR, MWRLIDAR, MFRSR, CIMEL, DOPPLER LIDAR. (T4-T8)

T.2.3. ACI from MWR, NEPHELOMETER, CIMEL, DOPPLER LIDAR. (T9-T12)

T.2.4. Use of Remote sensing for the characterization of aerosol changes due to cloud activation. (T3-T12)

Poster in European Lidar Conference (ELC2018):
 Synergic Combination of Active and Passive Remote Sensing Techniques for
 Investigating Aerosol-Cloud Interactions in Low-level Liquid Water Clouds: First
 Results Over the Southern Iberian Peninsula
 M. Castro-Santiago et al.

METHODOLOGY

1. Database:

- Years: 2012, 2013, 2017 (total: 10 months)
- Resolution: 1 minute
- Sun-photometer: COD (cloud optical depth), AOD (aerosol optical depth), $AE_{440-870}$ (Angström exponent)
- Ceilometer: CBH (cloud base height)
- Radiometer: LWP (liquid water path)
- Retrieved variables: Cloud Effective Radius (r_{eff}) and Droplet Number Concentration (N_d), (Painemal and Zuidema, 2011) [5]

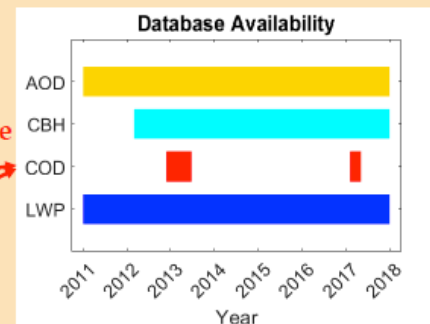
2. AOD inter- and extrapolation

- AOD variability slower than COD variability
- AOD interpolated or extrapolated at time of COD value (maximum ± 2 hours centered at COD time)

$$r_{eff} = \frac{9}{5} \frac{LWP}{\rho_w COD}$$

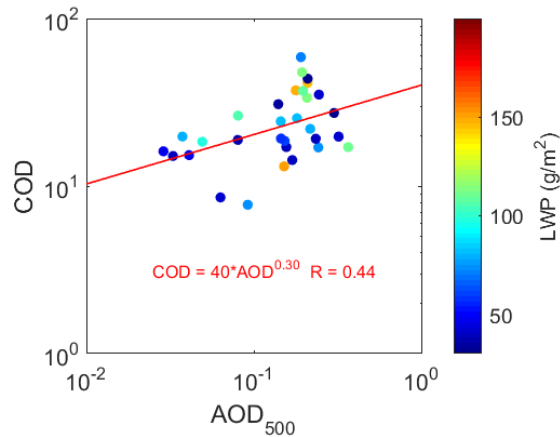
COD:
Limiting variable

$$N_d = 1,4067 \cdot 10^{-6} [cm^{-1}] \frac{COD^{1/2}}{r_{eff}^{5/2}}$$

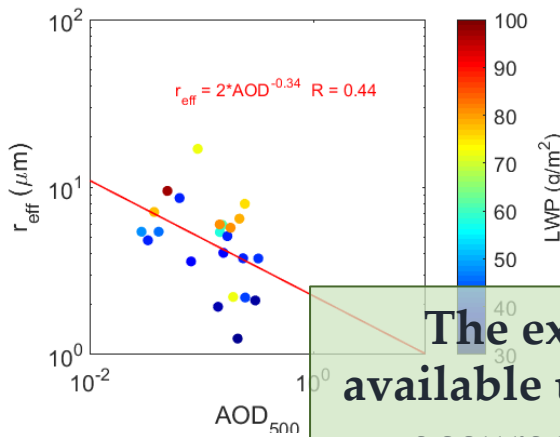


Criteria for data selection:

- Low altitude clouds: $CBH < 2000$ m a.g.l
- Opaque clouds: $COD > 5$
- Non-precipitating clouds: $LWP < 200$ g/m²
- $AE_{440-870} \geq 0$ and $AE_{440-870} \leq 2$

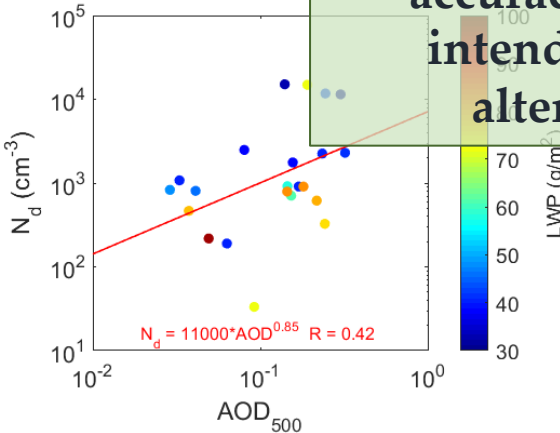


- COD values with LWP between 30 and 200 g/m² are plotted versus AOD
- A positive correlation is found
- $ACI_{COD} = 0.30$, consistent with theoretical interval (0-0.33)



- r_{eff} values with LWP between 30 and 100 g/m² are plotted versus AOD
- A negative correlation is found.
- A more narrow LWP interval is needed since r_{eff} is calculated with it

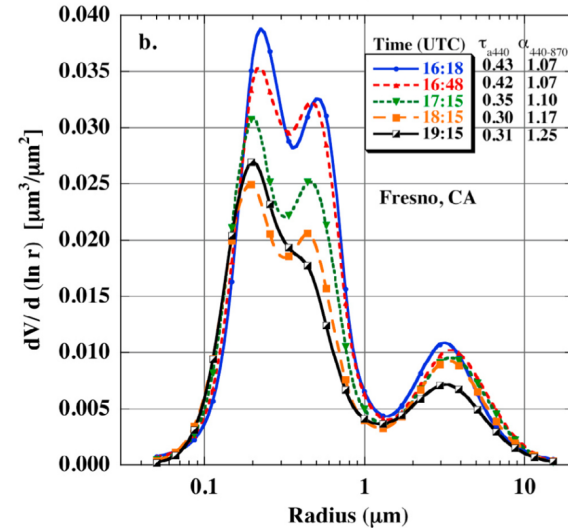
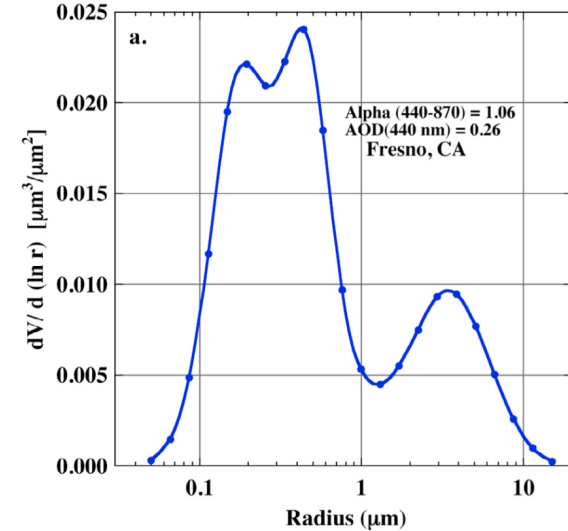
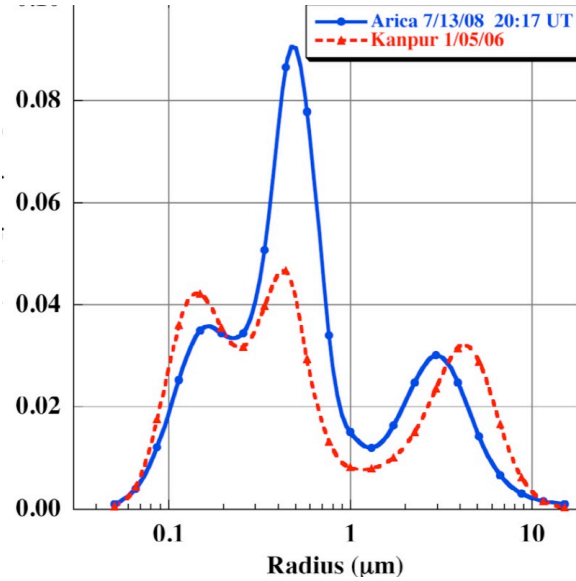
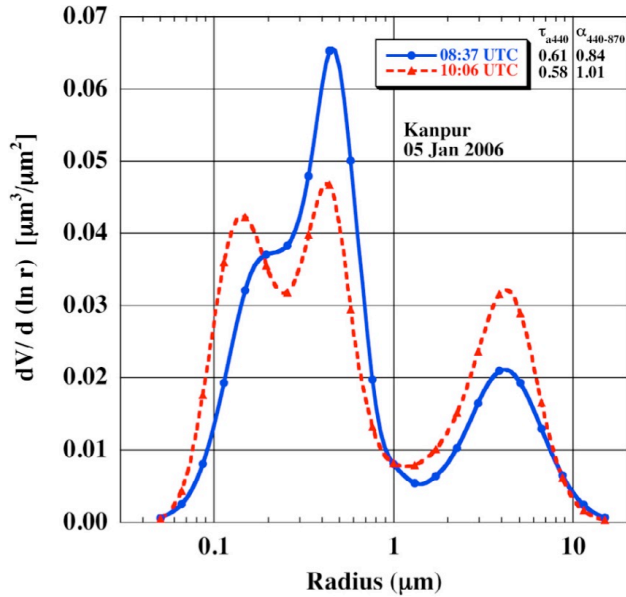
The extremely low number of COD measurements available up to the date at Granada has greatly limited the accuracy of ACI indexes calculated. This database is intended to be increased with COD retrieved with alternative methods (e.g. MFRSR7, MODIS...)



- N_d values with LWP between 30 and 100 g/m² are plotted versus AOD
- A positive correlation is found
- Also a narrow LWP interval is chosen
- $ACI_{Nd} = 0.85$, consistent with theoretical interval (0-1)

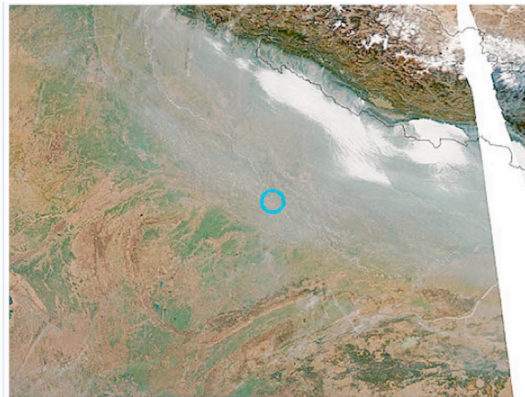
Analyzing the cloud-induced aerosol modifications by combination of remote sensing techniques

Eck, T. F., et al. (2012) J. Geophys. Res., 117, D07206, doi:10.1029/2011JD016839



MODIS Images: 2000m 1000m 500m 250m

TERRA-MODIS Granule Overpass Time:

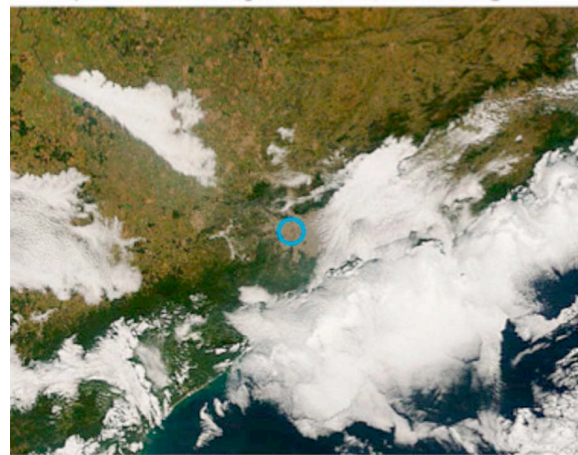
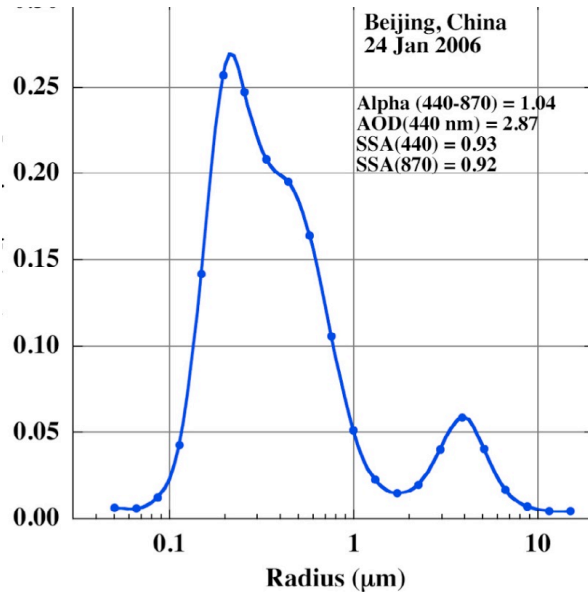


MODIS Images: 2000m 1000m 500m 250m

AQUA-MODIS Granule Overpass Times:

Analyzing the cloud-induced aerosol modifications by combination of remote sensing techniques

Eck, T. F., et al. (2012) J. Geophys. Res., 117, D07206, doi:10.1029/2011JD016839



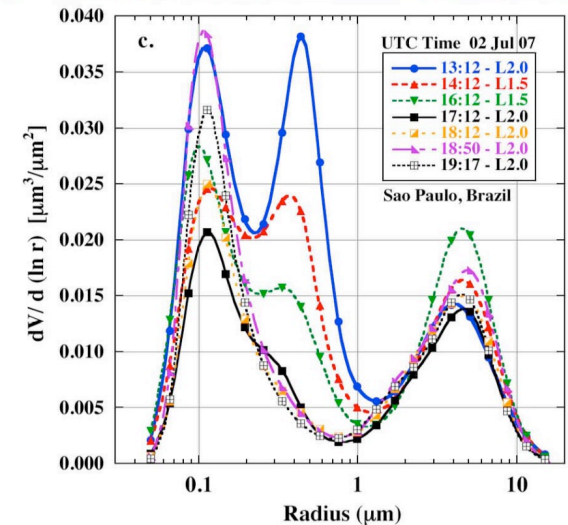
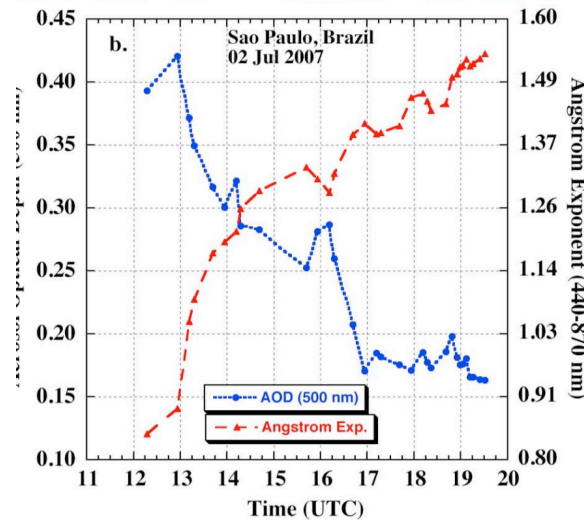
MODIS Images: 2000m 1000m 500m 250m

TERRA-MODIS Granule Overpass Time:
13:00 UTC



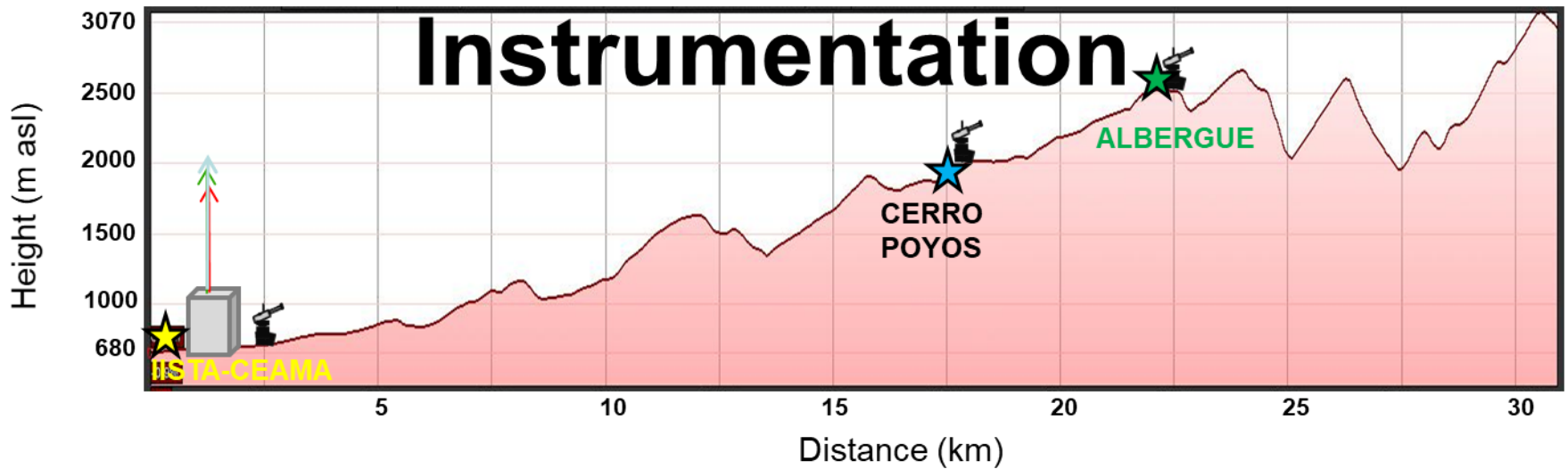
MODIS Images: 2000m 1000m 500m 250m

AQUA-MODIS Granule Overpass Times:
17:20, 17:25 UTC



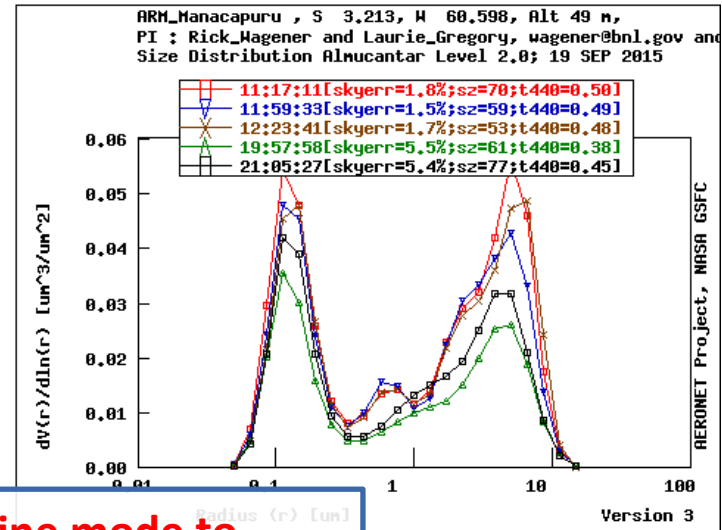
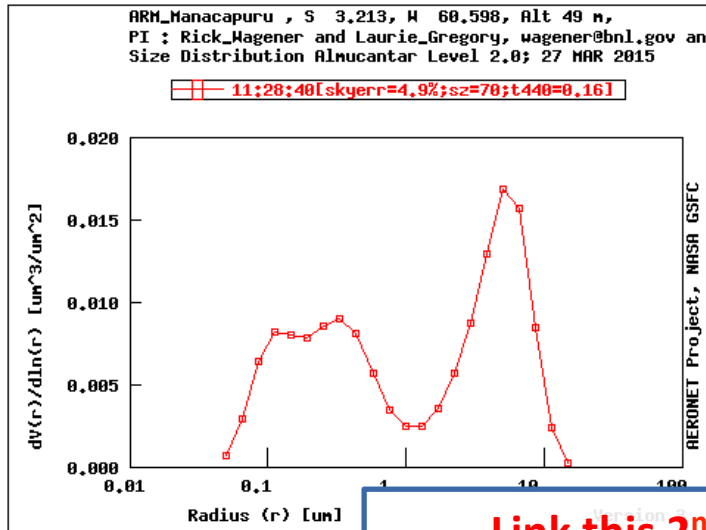
Analyzing the cloud-induced aerosol modifications by combination of remote sensing techniques

STATION: ARM_MANACAPURU	PERIOD: 01/01/2013-31/12/2015	PSD: 37
STATION: MANAUS_EMBRAPA	PERIOD: 01/01/2011-31/07/2018	PSD: 48
STATION: GRANADA	PERIOD: 01/01/2004-31/07/2018	PSD: 114
STATION: CERRO POYOS	PERIOD: 01/01/2004-31/07/2018	PSD: 21
STATION: ALBERGUE_UGR	PERIOD: 01/01/2016-31/07/2018	PSD: 0

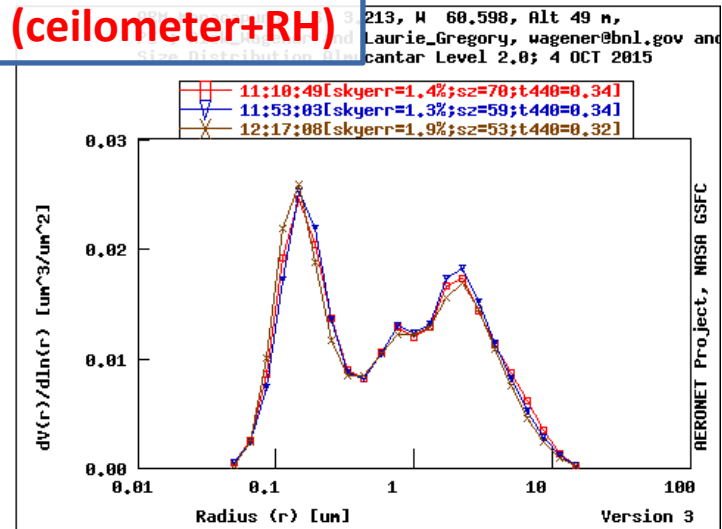
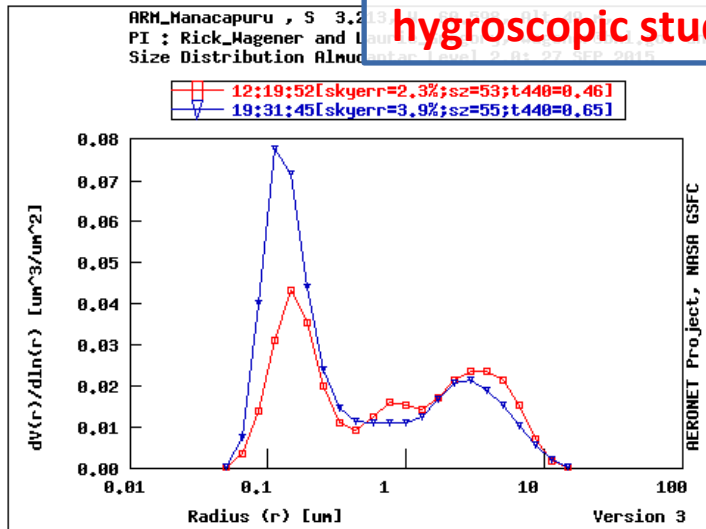


Analyzing the cloud-induced aerosol modifications by combination of remote sensing techniques

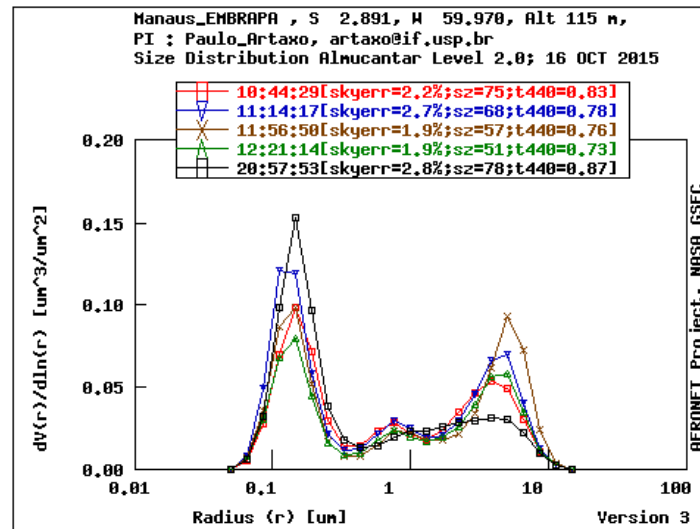
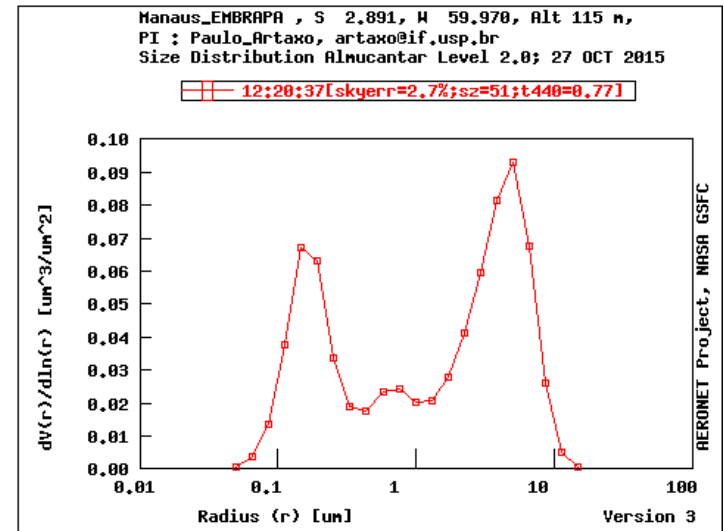
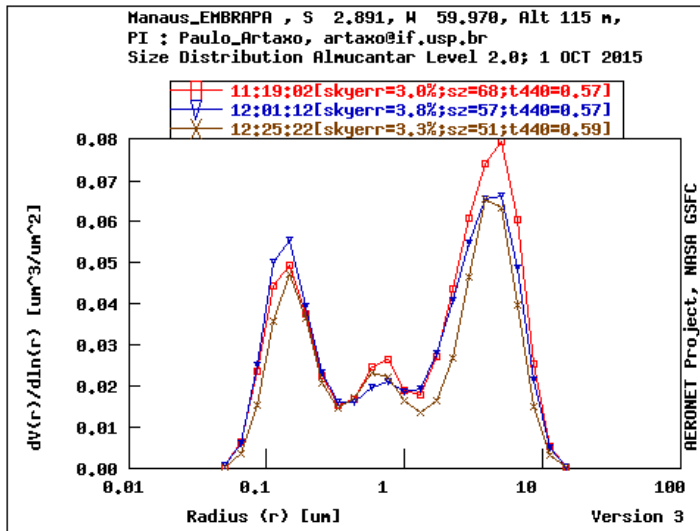
ARM_Manacapuru



Link this 2nd fine mode to
hygroscopic study (ceilometer+RH)

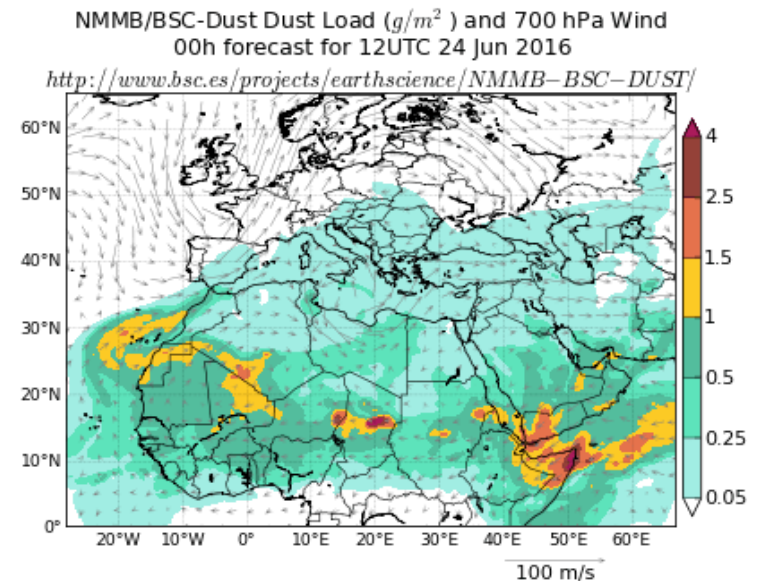
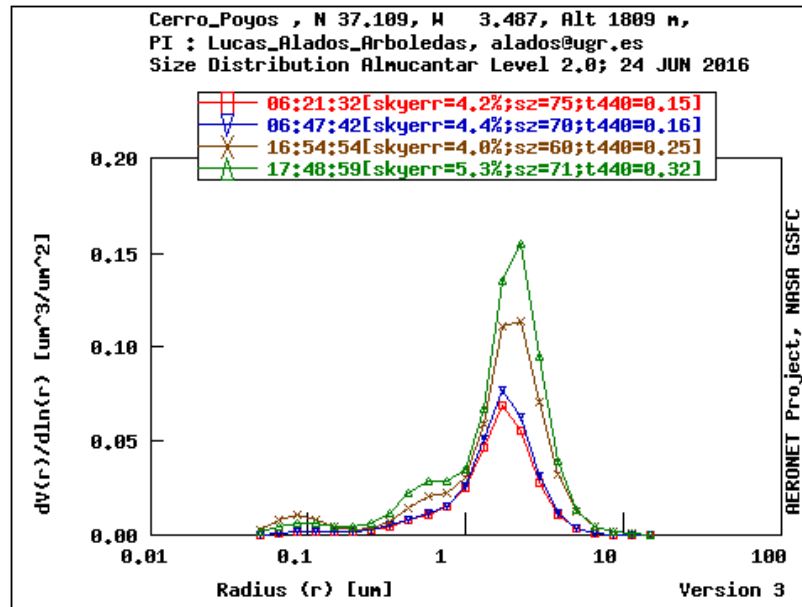


Analyzing the cloud-induced aerosol modifications by combination of remote sensing techniques



Analyzing the cloud-induced aerosol modifications by combination of remote sensing techniques

Cerro_Poyos



One future project...

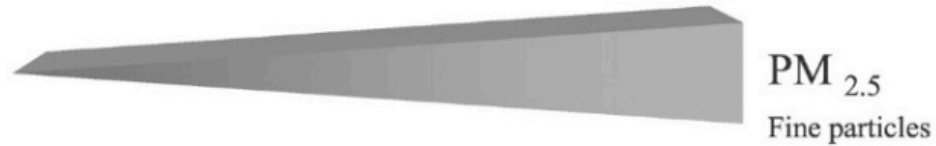
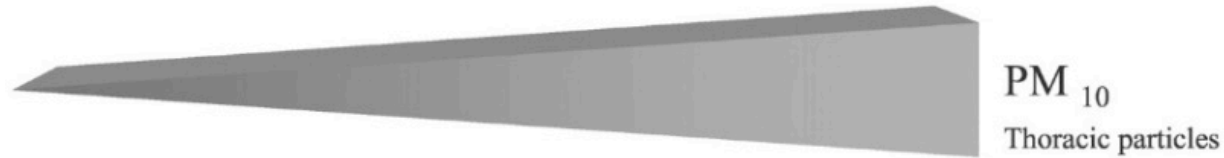
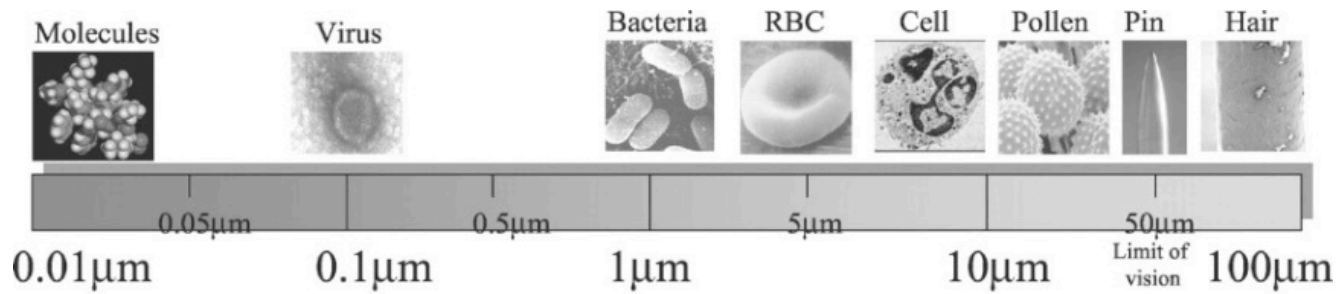




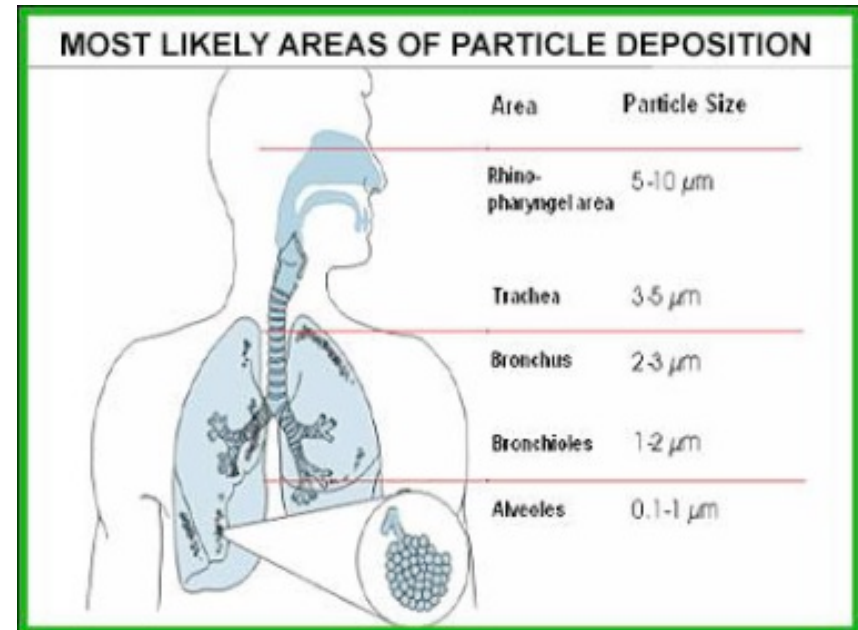
Preliminar title: Study of the vertical distribution of pollen grains and their potential transport by combination of in-situ and remote sensing techniques

AEROBIOLOGY: Discipline of Biology that studies the organic particles that are transported passively through the air. It includes viruses, bacteria, fungal spores, small insects and **pollen grains**

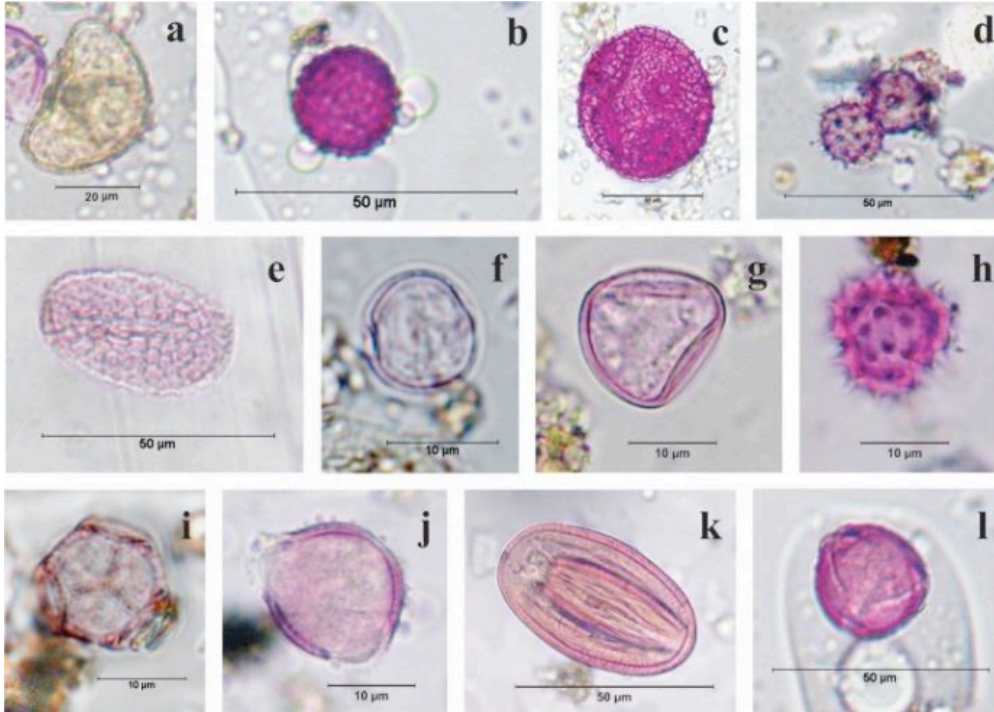
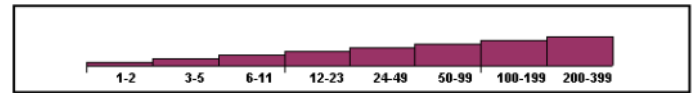
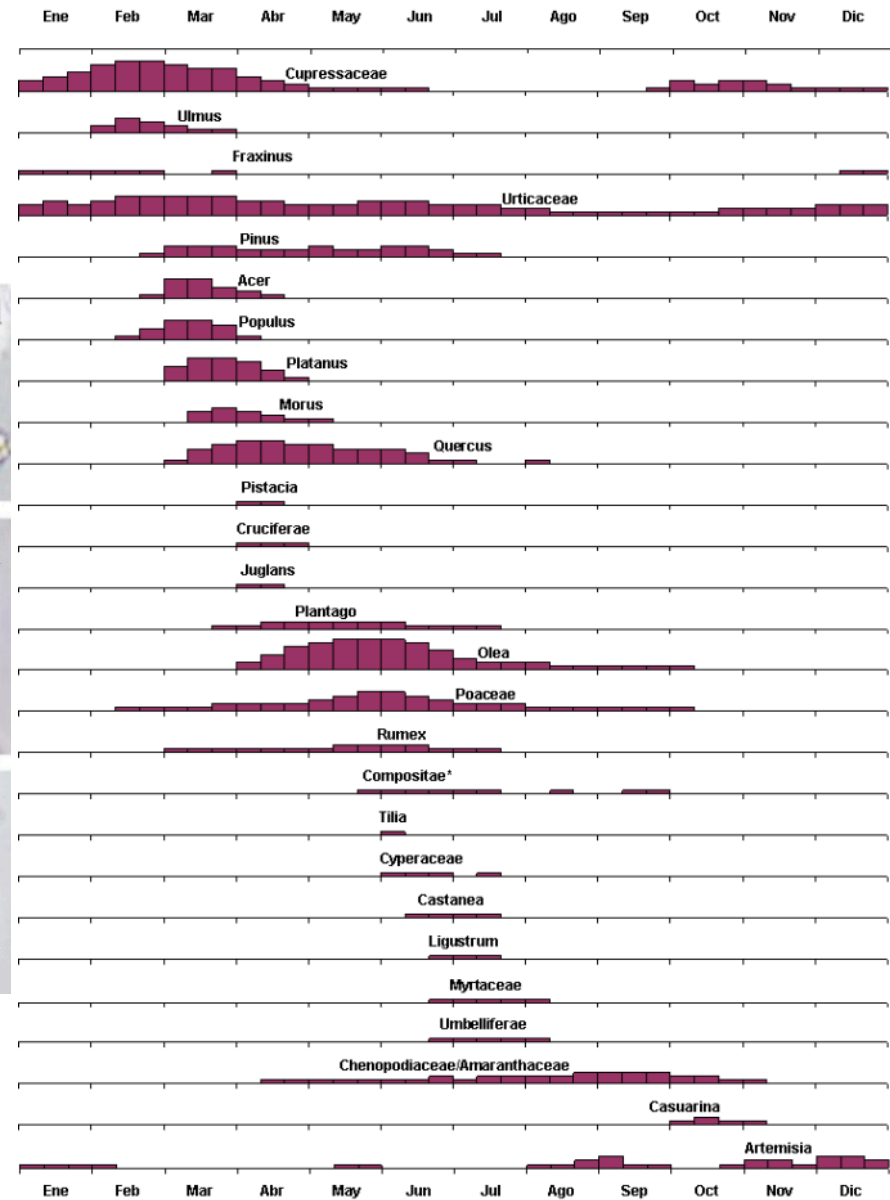
BPM: Biological Particulate Matter [[Cariñanos et al., 2016](#)]



(diameter)



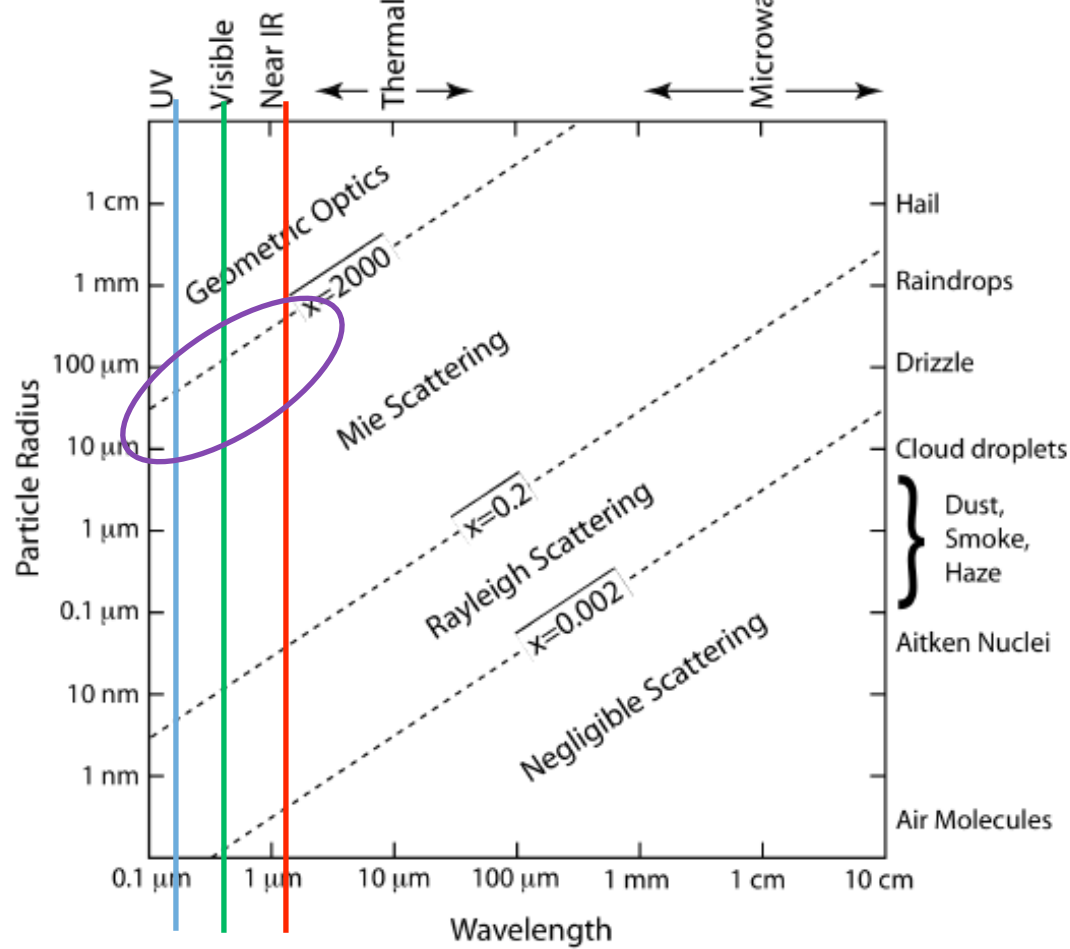
Typical pollen grains observed at Granada



Is it possible to detect pollen grains with remote sensing systems?

Polen:
 $1.25 \mu\text{m} < r < 125 \mu\text{m}$

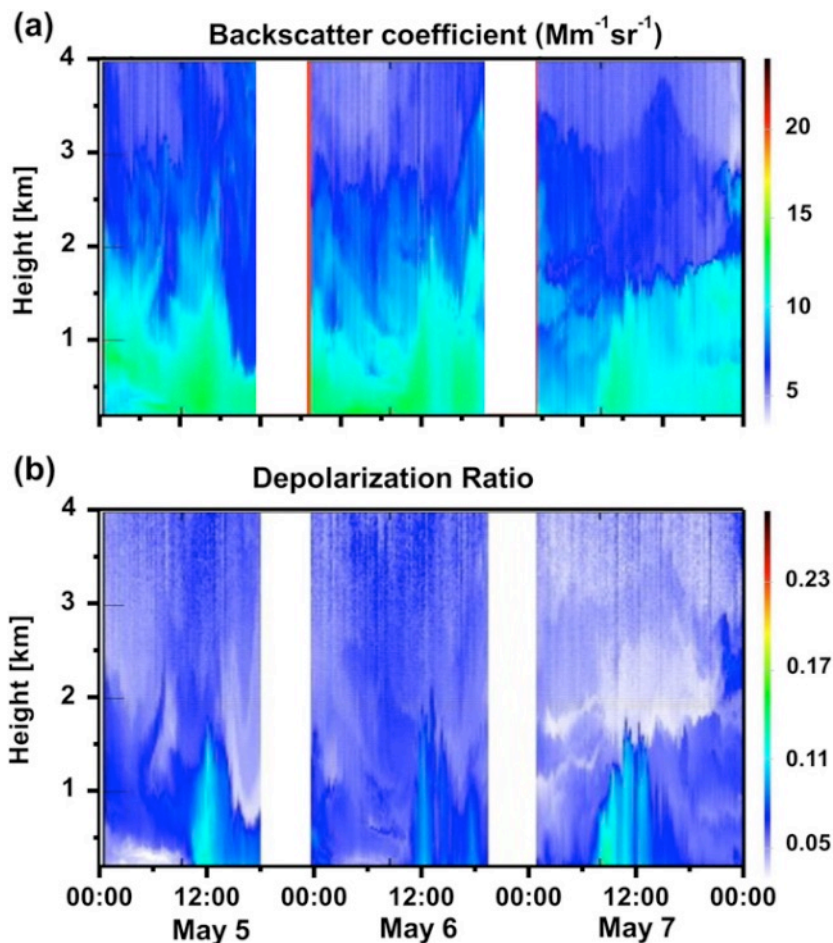
Mainly:
 $10 \mu\text{m} < r < 25 \mu\text{m}$



Scattering regimes related to the Particle size and Wavelength (Kostylev, 2007)

V. I. Kostylev, "Scattering Fundamentals," *Bistatic Radar Principles Practice*, pp. 193–223, 2007

From lidar measurements...



Contour plots of backscatter coefficient (a) and linear volume depolarization ratio (b) measured by the depolarization lidar system from May 5 (00:00 LT) to May 7 (24:00 LT) 2009.

Noh et al., Atmospheric Environment 69 (2013) 139- 147

Assuming that there are only two aerosol types, i.e. non-spherical and spherical particles in an air mass, and they are externally mixed.

Contribution ratio, $R_N(z)$, of the non-spherical particle backscattering coefficient to the total backscatter coefficient (Shimizu et al., 2004):

retrieved part. depol. Ratio
(spherical+non-spherical)

$$R_N(z) = \frac{(\delta_p(z) - \delta_2)(1 + \delta_1)}{(\delta_1 - \delta_2)(1 + \delta_p(z))}$$

Input: non-spherical
depol.ratio

Input: spherical
depol.ratio

For pollen:

$$R_p(z) = R_N(z) - R_a(z)$$

$$\beta_p(z) = R_p(z)\beta_a(z)$$

Open issues...

retrieved part. depol. Ratio
(spherical+non-spherical)

$$R_N(z) = \frac{(\delta_p(z) - \delta_2)(1 + \delta_1)}{(\delta_1 - \delta_2)(1 + \delta_p(z))}$$

Input: non-spherical
depol.ratio

Input: spherical
depol.ratio

- ❑ δ_1 (pollen depol. ratio) is unknown. Typically, a value of 0.34 (Pure Saharan dust) is used
- ❑ δ_p retrieved using Klett method during daytime: pollen lidar ratio is unknown. Typically, a value of 50 sr is used
- ❑ δ_p retrieved using Klett method during daytime: need to improve overlap and/or daytime Raman measurements (rotational Raman filters)

WG1. In situ techniques: fluorescence, Hirst sampler & laboratory analyses

- Comparison fluorescence system vs Hirst sampler
- Determination of periods with high pollen concentration
- Pollen sampling for laboratory analysis in the University of Hertfordshire
- Optical analysis of pollen samples to obtain LR_{pollen} y δ_{pollen} for predominant pollen types
- Short stays in the University of Hertfordshire (England) & University of Granada (Spain)

WG2. Remote sensing techniques: lidar & Sun-photometer

- Comparison Sun-phot. vs Hirst sampler (and/or fluorescence system): investigating cases of wrong attribution to clouds or mineral dust
- Improvement of overlap function (intensive application of traditional retrieving method, use of rotational Raman filters, overlap at 1064 nm, new methods by combination with MWR or RS)
- Characterization of the pollen vertical distribution during special events
- Analysis of regional-transport of pollen
- Short stays in the University of Évora (Portugal) & University of Granada (Spain)

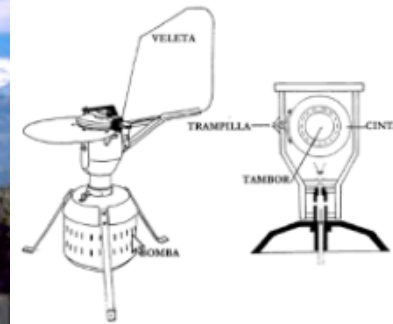
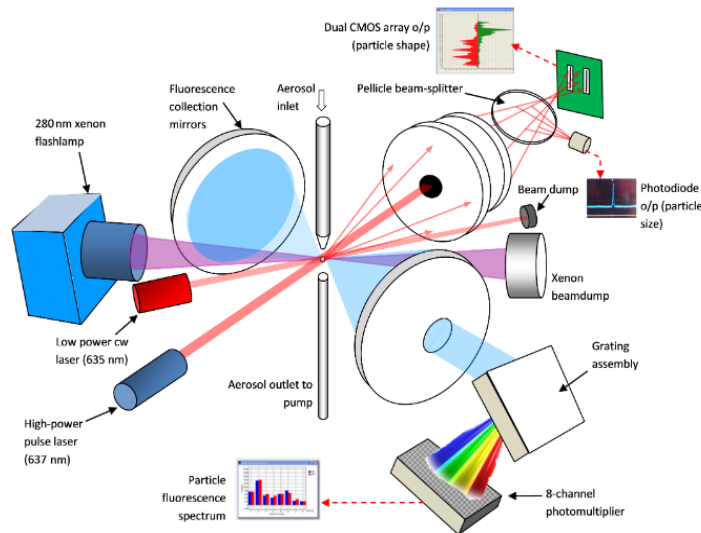
WG3. Dissemination of results

- Articles
- Contributions to congresses (ILRC, ELC, WLMLA, EAC, RICTA...)
- Web



WG1. In situ techniques: fluorescence, Hirst sampler & laboratory analyses

- Comparison fluorescence system vs Hirst sampler
- Determination of periods with high pollen concentration
- Pollen sampling for laboratory analysis in the University of Hertfordshire
- Optical analysis of pollen samples to obtain LR_{pollen} y δ_{pollen} for predominant pollen types
- Short stays in the University of Hertfordshire (England) & University of Granada (Spain)



Scheme of *Multiparameter Bioaerosol Spectrometer (MBS)* [Ruske et al., 2017]

- ❑ Information on scattering pattern (related to size and shape) and fluorescence of individual particles
- ❑ Record fluorescence in 8 bands between 310-640 nm
- ❑ 2 CMOS detectors of 512 pixels
- ❑ Characterization of bacteria, pollen, spores, fungi, etc. in real time

Hirst-type volumetric pollen sampler, LANZONI VPPS 2000

- ❑ working under the principle of impact by suction
- ❑ Constant volume of 10 litre/min
- ❑ Hourly measurements (pollen grains/m³)

WG1. In situ techniques: fluorescence, Hirst sampler & laboratory analyses

- Comparison fluorescence system vs Hirst sampler
- Determination of periods with high pollen concentration
- Pollen sampling for laboratory analysis in the University of Hertfordshire
- Optical analysis of pollen samples to obtain LR_{pollen} y δ_{pollen} for predominant pollen types
- Short stays in the University of Hertfordshire (England) & University of Granada (Spain)

Lidar spectroscopy instrument (LiSsI):

It will enable profiling of trace gases, chemical components in particles, and **bio-aerosols** in atmospheric aerosol pollution in the troposphere through combining different non-linear spectroscopy techniques (photoluminescence, fluorescence, Raman and coherent anti-Stokes Raman spectroscopy) in a single measurement platform



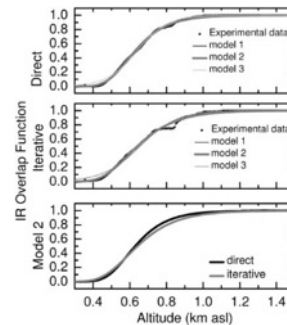
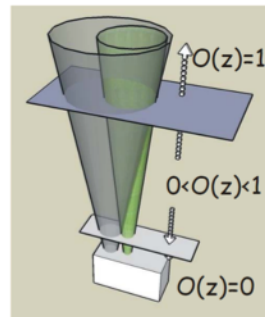
Table 1. Technical specification of the receiver and data acquisition systems

Continuum Powerlite Furie LD		Horizon Optical Parametric Oscillator	
Laser type	Nd:YAG, injection seeded	Pump wavelength	355 nm
Pulse energy	7500 mJ@1064 nm 5000 mJ@532 nm 2500 mJ@355 nm	Wavelengths	from 192 to 2750 nm scan step 0.01 nm
Beam divergence	0.5 mrad	Pulse energy	120 mJ@400 nm 60 mJ@600 nm 25mJ@300 nm
Repetition rate	10 Hz	Beam divergence	<2 mrad (both axes)
Linewidth	<0.003 cm ⁻¹	Repetition rate	10 Hz
Pulse duration	<15 ns		
HORIBA 1250M Research Spectrometer		Detection	
Focal length	1.25 m, F/9	Mie and Rayleigh scattering	355 nm, PMT HV-R9880U-20 532 nm, PMT HV-R9880U-20 1064 nm, APD InGaAs50, Si
Spectral range	0-1500 nm @ 1200 g/mm	Spectroscop. 1 Licel SP32-20	Hamamatsu H7260-20, 0.8 mm x 7 mm x 32 anodes spectral response 300-920 nm
Grating size	110 mm x 110 mm		
Dispersion @500 nm	0.65 nm/mm	Spectroscop. 2 Princeton Instruments PI-MAX4 ICCD camera	1024x1024 pixels 12.8 x 12.8 μm pixels Gen III filmless intensifier Sensitive range 290-710 nm
Accuracy/Repeatability	±0.15 nm / ±0.005 nm		
Gratings and max resolutions @313.183 nm	2400 gr/mm @250 nm, resol. 0.003 nm		
	1800 gr/mm @ 400 nm, resol. 0.004 nm 1200 gr/mm @ 330 nm, resol. 0.006 nm 600 gr/mm @ 500 nm, resol. 0.012 nm		
		Schmidt-Cassegrain telescope	
		Focal length	3910 mm (14 inch)
		Field of view	0.5-4.0 mrad (variable)
Data acquisition system			
Mie and Rayleigh scattering	Licel transient recorders, 16 bit, 20 MHz A/D converters and photon-counters maximum count rate 250 MHz		
Multi-anode PMT	Single-photon counting, maximum count rate 100 MHz, 50 ns resolution		
ICCD	Digitization 16 bit, 32 MHz, minimum gate width 2 ns		



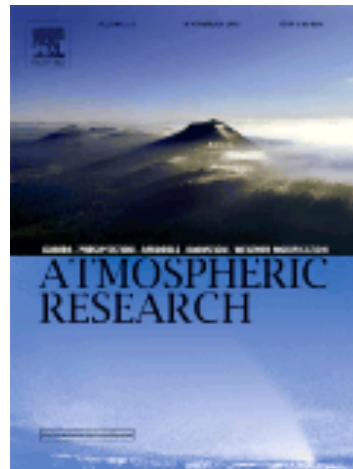
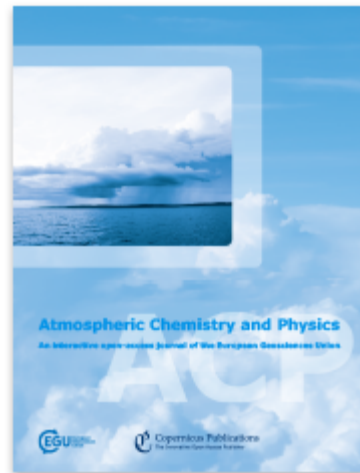
WG2. Remote sensing techniques: lidar & Sun-photometer

- Comparison Sun-phot. vs Hirst sampler (and/or fluorescence system): investigating cases of wrong attribution to clouds or mineral dust
- Improvement of overlap function (intensive application of traditional retrieving method, use of rotational Raman filters, overlap at 1064 nm, new methods by combination with MWR or RS)
- Characterization of the pollen vertical distribution during special events
- Analysis of regional-transport of pollen
- Short stays in the University of Évora (Portugal) & University of Granada (Spain)



WG3. Dissemination of results

- Articles
- Contributions to congresses (ILRC, ELC, WLMLA, EAC, RICTA...)
- Web



Exchange of knowledge



Calls for exchange:

- Fundación Carolina: postgraduate scholarships, PhD scholarships, short-stay scholarships, Brazilian professors (duration: variable)

<https://www.fundacioncarolina.es>

- ACTRIS Transnational Access (TNAs): students, technicians, researchers & professors (~days, typically maximum 1 month)

<https://www.actris.eu/DataServices/ObservationalFacilities/AccessToObservationalFacilities.aspx>

- IISTA-CEAMA visitors program: researchers & professors (max: 1 week)

link: coming soon

- UGR call for short stays (P11): researchers & professors (min 1 month, max 3 months)

<https://investigacion.ugr.es/pages/planpropio/2018/normas/p11>

- UGR call “CAPTACIÓN DE TALENTO EN GRADOS UNIVERSITARIOS” (P26): undergraduated students (1 month, July, only accommodation and meals)

<https://investigacion.ugr.es/pages/planpropio/2018/normas/p26>



... muito obrigado